

LEVERAGING CHRISTOFFEL-DARBOUX KERNELS TO STRENGTHEN MOMENT-SOS RELAXATIONS

SREĆKO ĐURAŠINOVIĆ^{1,2}, PERLA AZZI¹, JEAN-BERNARD LASSERRE^{3,4}, VICTOR MAGRON^{3,5},
OLGA MULA⁶, AND JUN ZHAO²

ABSTRACT. The classical Moment-Sum Of Squares hierarchy allows to approximate a global minimum of a polynomial optimization problem through semidefinite relaxations of increasing size. However, for many optimization instances, solving higher order relaxations becomes impractical or even impossible due to the substantial computational demands they impose. To address this, existing methods often exploit intrinsic problem properties, such as symmetries or sparsity. Here, we present a complementary approach, which enhances the accuracy of computationally more efficient low-order relaxations by leveraging Christoffel-Darboux kernels. Such strengthened relaxations often yield significantly improved bounds or even facilitate minimizer extraction. We illustrate the efficiency of our approach on several classes of important quadratically constrained quadratic programs.

CONTENTS

1. Introduction	1
1.1. Notation	3
2. Main ingredients	3
2.1. The classical Moment-SOS hierarchy	3
2.2. Christoffel-Darboux kernels	6
3. Strengthening relaxation bounds	7
3.1. Iterative approach - H1	9
3.2. Local-solution-based approach - H2	12
4. Numerical Experiments	15
4.1. QCQP over $[0, 1]^n$	15
4.2. Exploiting correlative sparsity	19
4.3. Beyond QCQPs	21
5. Conclusion	22
Acknowledgements	23
References	23
Appendix	25

1. INTRODUCTION

Polynomial optimization revolves around minimizing or maximizing a polynomial over a basic closed semialgebraic set, i.e., a set corresponding to the conjunction of finitely many polynomial equalities and inequalities. Generally, these problems are NP-hard [16]. However, in [12], the author provided a way of approximating the global optimum of a polynomial optimization

(1) CNRS@CREATE LTD, SINGAPORE

(2) COLLEGE OF COMPUTING AND DATA SCIENCE, NANYANG TECHNOLOGICAL UNIVERSITY

(3) LAAS-CNRS

(4) TOULOUSE SCHOOL OF ECONOMICS

(5) INSTITUTE OF MATHEMATICS FROM TOULOUSE

(6) EINDHOVEN UNIVERSITY OF TECHNOLOGY, DEPARTMENT OF MATHEMATICS AND COMPUTER SCIENCE

E-mail addresses: SRECK0001@e.ntu.edu.sg, perla.azzi@cnrsatcreate.sg, lasserre@laas.fr, vmagron@laas.fr, o.mula@tue.nl, junzhao@ntu.edu.sg.

problem (POP) by a hierarchy of semidefinite programming (SDP) relaxations. Finite convergence guarantees, under mild conditions, were later derived in [22]. We refer the reader to [6, 19, 24] and references therein for a detailed analysis of the hierarchy and its use in real-life applications.

The main bottleneck of the proposed hierarchy, often called *Moment-Sum of Squares* (Moment-SOS for short) or *Lasserre's hierarchy*, is its scalability. Indeed, this hierarchy involves semidefinite positive constraints on matrices of size up to $\binom{n+d}{d}$, where n is the ambient space dimension and d is the relaxation order, rendering it intractable if either of these parameters is large. While it is true that $\binom{n+d}{d} = \mathcal{O}(n^d)$ for a fixed n , the curse of dimensionality becomes apparent when attempting to solve higher order relaxations with state-of-the-art SDP solvers. Fortunately, many POP instances possess intrinsic structural properties whose adequate exploitation can lead to an increase in computational efficiency and mitigate the curse of dimensionality.

For example, more efficient relaxations that exploit *symmetries* were introduced in [28]. Furthermore, detecting and taking advantage of the problem's *sparsity* constitutes another important direction in this domain, where some of the commonly studied sparsity patterns are *correlative sparsity* [31, 14], *term sparsity* [33, 34] and *ideal sparsity* [9].

Alternatively, one may try to identify some additional properties of the problem and translate them into new constraints. These new constraints, when coupled with the initial ones, often produce tighter relaxation bounds at each step of the hierarchy. For instance, strengthening the first-order moment relaxations by adding redundant quadratic constraints has been studied in [35]. In [23], the author derives additional constraints involving *Lagrange multipliers* associated to the original problem. These multipliers are represented as polynomials in the initial decision variables, and the proposed approach is demonstrated to provide better relaxation bounds whenever the optimal value is attained at a critical point of the associated Lagrangian. Combining correlative sparsity and Lagrange multiplier expressions is presented in [27]. In [4], the authors propose a dynamic inequality generation scheme to construct valid polynomial inequalities. Strengthened relaxation bounds using *shift* and *multiplication* operators, which arise when one tries to express optimality conditions of a given POP in a positive semidefinite manner, are obtained in [32]. One common drawback of the last two above-mentioned approaches is that they require to solve auxiliary relaxations at higher orders.

Contribution. We introduce a complementary approach leveraging Christoffel-Darboux kernels. Recent works, such as [25, 11], have demonstrated the broader applicability of these kernels, particularly in addressing data analysis challenges, paving the way for their use in optimization. In particular, results from [13], reveal a very deep connection between Christoffel-Darboux kernels and SOS polynomials, which are one of the main building blocks of the Moment-SOS hierarchy. Our main contribution lies in exploiting these insights for strengthening classical hierarchy bounds, namely:

- We argue that utilizing the Christoffel-Darboux kernel constructed at a fixed level d of the hierarchy enables the construction of specific polynomial constraints that effectively restrict the feasible set. This approach yields significant improvements in bounds without incurring the computational cost of solving often intractable higher-order relaxations. Furthermore, we present and analyze the properties of two distinct heuristics for constructing these additional constraints;
- We demonstrate the effectiveness of our approach on a variety of quadratically constrained quadratic programs (QCQPs) across different dimensions.

The rest of the paper is structured as follows: in Section 2, we recall some important properties of the main ingredients used in this paper: the Moment-SOS hierarchy and the Christoffel-Darboux kernels. In Section 3, we introduce two different heuristic methods based on Christoffel-Darboux kernels, aimed at strengthening the classical relaxation bounds. Finally, in Section

4, we illustrate the performance of both heuristics on various classes of QCQPs and provide guidelines on how to use these heuristics in practice for more general problems.

1.1. Notation. We use Roman letters to denote scalars, and boldfaced letters to represent vectors and matrices. Let $\mathbb{R}[\mathbf{x}] = \mathbb{R}[x_1, \dots, x_n]$ be the ring of real n -variate polynomials, where $\mathbf{x} = (x_1, \dots, x_n)$. For $d \in \mathbb{N}$, we denote by $\mathbb{R}_d[\mathbf{x}]$ the finite-dimensional space of polynomials of degree less than d , equipped with a standard monomial basis $\mathbf{v}_d := (1, x_1, \dots, x_n, x_1^2, \dots, x_n^d)$ of size $s(n, d) := \binom{n+d}{d}$. A positive semidefinite (PSD) matrix \mathbf{M} is denoted by $\mathbf{M} \succeq 0$, and the set of symmetric (resp. symmetric PSD) matrices of size n is denoted by \mathcal{S}^n (resp. \mathcal{S}_+^n).

Given $(d, n) \in \mathbb{N}^2$, we define the multi-index set $\mathbb{N}_d^n := \{\boldsymbol{\alpha} = (\alpha_1, \dots, \alpha_n) \in \mathbb{N}^n \mid \sum_{i=1}^n \alpha_i \leq d\}$. Consequently, given $\mathbf{x} \in \mathbb{R}^n$ and $f \in \mathbb{R}_d[\mathbf{x}]$, we will often write $f(\mathbf{x}) = \sum_{\boldsymbol{\alpha} \in \mathbb{N}_d^n} f_{\boldsymbol{\alpha}} \mathbf{x}^{\boldsymbol{\alpha}}$ with $f_{\boldsymbol{\alpha}} \in \mathbb{R}$, $\mathbf{x}^{\boldsymbol{\alpha}} = x_1^{\alpha_1} \dots x_n^{\alpha_n}$. The support of f is $\text{supp}(f) := \{\boldsymbol{\alpha} \in \mathbb{N}^n \mid f_{\boldsymbol{\alpha}} \neq 0\}$.

The set of real-valued sequences indexed by elements of a set S is denoted by \mathbb{R}^S . The set of finite signed Borel measures (resp. positive finite Borel measures) supported on a set K is denoted by $\mathcal{M}(K)$ (resp. $\mathcal{M}_+(K)$). We denote by $\mathbb{1}_S$ the indicator function of the set S .

2. MAIN INGREDIENTS

2.1. The classical Moment-SOS hierarchy. Let $f \in \mathbb{R}[\mathbf{x}]$ and $m \in \mathbb{N}^*$ such that $g_1, \dots, g_m \in \mathbb{R}[\mathbf{x}]$. Let K be a basic closed semialgebraic set defined by

$$(1) \quad K := \{\mathbf{x} \in \mathbb{R}^n \mid g_1(\mathbf{x}) \geq 0, \dots, g_m(\mathbf{x}) \geq 0\}.$$

Let us consider the general Polynomial Optimization Problem (POP) of the form:

$$(2) \quad \mathbf{P} : \quad f_{\min} = \inf_{\mathbf{x} \in K} f(\mathbf{x}).$$

Optimization problems of this type are generally nonlinear and nonconvex, which makes them very difficult to solve. However, one effective tool for tackling these problems is the Lasserre's hierarchy [12]. The essence of Lasserre's hierarchy lies in transforming the initial problem into a hierarchy of finite-dimensional primal-dual semidefinite programming (SDP) problems. The primal problem revolves around characterizing moment sequences of Borel measures, forming a *moment problem*. On the other hand, the dual problem involves describing positive polynomials that admit weighted sum of squares (SOS) decompositions, where the weights are the polynomials g_j involved in the description of K .

We recall that a polynomial $f \in \mathbb{R}_{2d}[\mathbf{x}]$ is said to be SOS if there exist $k \in \mathbb{N}^*$ and $p_1, \dots, p_k \in \mathbb{R}_d[\mathbf{x}]$ such that $f = p_1^2 + \dots + p_k^2$. Moreover, if f is SOS, then there exists a matrix $\mathbf{G} \in \mathcal{S}_+^{s(n,d)}$, called *Gram matrix*, such that $f = \mathbf{v}_d^\top \mathbf{G} \mathbf{v}_d$.

Let $\mathbf{y} = (y_{\boldsymbol{\alpha}})_{\boldsymbol{\alpha} \in \mathbb{N}^n}$ be a real-valued sequence. We can always associate to \mathbf{y} the linear *Riesz functional* $L_{\mathbf{y}}$ defined as follows:

$$L_{\mathbf{y}} : \mathbb{R}[\mathbf{x}] \ni f \mapsto L_{\mathbf{y}}(f) := \sum_{\boldsymbol{\alpha} \in \text{supp}(f)} f_{\boldsymbol{\alpha}} y_{\boldsymbol{\alpha}} \in \mathbb{R}.$$

For $d \in \mathbb{N}$, the symmetric matrix $\mathbf{M}_d(\mathbf{y})$ of size $s(n, d)$ is called the *pseudo-moment matrix* of order d associated with \mathbf{y} , and its entry $(\boldsymbol{\alpha}, \boldsymbol{\beta})$ is given by:

$$(3) \quad \mathbf{M}_d(\mathbf{y})(\boldsymbol{\alpha}, \boldsymbol{\beta}) := L_{\mathbf{y}}(\mathbf{x}^{\boldsymbol{\alpha}} \mathbf{x}^{\boldsymbol{\beta}}) = y_{\boldsymbol{\alpha} + \boldsymbol{\beta}}, \quad \boldsymbol{\alpha}, \boldsymbol{\beta} \in \mathbb{N}_d^n.$$

Similarly, for $g \in \mathbb{R}[\mathbf{x}]$, the symmetric matrix $\mathbf{M}_d(g\mathbf{y})$ represents the *localizing matrix* of order d associated with g and \mathbf{y} , defined as follows:

$$(4) \quad \mathbf{M}_d(g\mathbf{y})(\boldsymbol{\alpha}, \boldsymbol{\beta}) := L_{\mathbf{y}}(g\mathbf{x}^{\boldsymbol{\alpha}} \mathbf{x}^{\boldsymbol{\beta}}) = \sum_{\boldsymbol{\gamma} \in \text{supp}(g)} g_{\boldsymbol{\gamma}} y_{\boldsymbol{\alpha} + \boldsymbol{\beta} + \boldsymbol{\gamma}}, \quad \boldsymbol{\alpha}, \boldsymbol{\beta} \in \mathbb{N}_{d - \lceil \text{deg}(g)/2 \rceil}^n.$$

In particular, the localizing matrix of order d associated with the constant polynomial $g_0 = 1$ is the moment matrix of order d .

Casting the POP as a moment problem follows from the following observation:

$$(5) \quad \begin{aligned} f_{\min} &= \inf_{\mu \in \mathcal{M}_+(K)} \left\{ \int_{\mathbb{R}^n} f(\mathbf{x}) d\mu(\mathbf{x}) \mid \mu(K) = 1 \right\} \\ &= \inf_{\mathbf{y} \in \mathbb{R}^{N^n}} \left\{ L_{\mathbf{y}}(f) \mid \exists \mu \in \mathcal{M}_+(K), y_0 = 1, y_{\alpha} = \int_{\mathbb{R}^n} \mathbf{x}^{\alpha} d\mu(\mathbf{x}), \alpha \in \mathbb{N}^n \setminus \{\mathbf{0}\} \right\}. \end{aligned}$$

Indeed, suppose that $\mathbf{x}^* \in \mathbb{R}^n$ is a global minimizer of f over K , and consider the Dirac measure $\mu^* = \delta_{\mathbf{x}^*}$. Then, μ^* is feasible for the optimization problem over measures in (5), and

$$\int_{\mathbb{R}^n} f(\mathbf{x}) d\mu^*(\mathbf{x}) = f(\mathbf{x}^*) = f_{\min}, \text{ implying that } \inf_{\mu \in \mathcal{M}_+(K)} \left\{ \int_{\mathbb{R}^n} f(\mathbf{x}) d\mu(\mathbf{x}) \mid \mu(K) = 1 \right\} \leq f_{\min}.$$

Conversely, let μ be feasible in (5). Since for all $\mathbf{x} \in K$, $f(\mathbf{x}) \geq f_{\min}$, we obtain $\int_{\mathbb{R}^n} f(\mathbf{x}) d\mu(\mathbf{x}) \geq$

$$\int_{\mathbb{R}^n} f_{\min} d\mu(\mathbf{x}) = f_{\min}, \text{ implying that } \inf_{\mu \in \mathcal{M}_+(K)} \left\{ \int_{\mathbb{R}^n} f(\mathbf{x}) d\mu(\mathbf{x}) \mid \mu(K) = 1 \right\} \geq f_{\min}.$$

Equality between f_{\min} and the sequence-based reformulation in (5) can be established in a similar way.

The measure μ in the last line of expression (5) is referred to as the *representing measure* of \mathbf{y} .

This reformulated optimization problem, while linear in \mathbf{y} , remains infinite-dimensional because it requires all possible moments of the measure μ to match the elements of the sequence \mathbf{y} .

However, the next result provides a way to relax this problem into a finite-dimensional one. For each $j \in \{1, \dots, m\}$, let us define $d_j := \lceil \deg(g_j)/2 \rceil$ and $d_{\min} := \max \{ \lceil \deg(f)/2 \rceil, d_1, \dots, d_m \}$.

Proposition 2.1. *If $\mathbf{y} \in \mathbb{R}^{N_{2d}^n}$ is represented by a measure supported on the set K , then*

- (1) $\mathbf{M}_d(\mathbf{y}) \in \mathcal{S}_+^{s(n,d)}$,
- (2) $\mathbf{M}_{d-d_j}(g_j \mathbf{y}) \in \mathcal{S}_+^{s(n,d-d_j)}$, $j \in \{1, \dots, m\}$.

Proof. Let $\mu \in \mathcal{M}_+(K)$ such that $y_{\alpha} = \int_K \mathbf{x}^{\alpha} d\mu(\mathbf{x})$, for all $\alpha \in \mathbb{N}_{2d}^n$. Then, for any $\mathbf{p} \in \mathbb{R}^{s(n,d)}$,

$$(6) \quad \mathbf{p}^{\top} \mathbf{M}_d(\mathbf{y}) \mathbf{p} = L_{\mathbf{y}}(p^2) = \int_K p^2(\mathbf{x}) d\mu(\mathbf{x}) \geq 0 \implies \mathbf{M}_d(\mathbf{y}) \in \mathcal{S}_+^{s(n,d)}.$$

Similarly, for any $j \in \{1, \dots, m\}$, we have $\mathbf{M}_{d-d_j}(g_j \mathbf{y}) \in \mathcal{S}_+^{s(n,d-d_j)}$ since for any $\mathbf{p} \in \mathbb{R}^{s(n,d-d_j)}$,

$$(7) \quad \mathbf{p}^{\top} \mathbf{M}_{d-d_j}(g_j \mathbf{y}) \mathbf{p} = L_{\mathbf{y}}(p^2 g_j) = \int_K p^2(\mathbf{x}) g_j(\mathbf{x}) d\mu(\mathbf{x}) \geq 0.$$

□

Proposition (2.1) facilitates constructing a hierarchy of moment relaxations for problem \mathbf{P} [12]. Namely, the *moment relaxation* for the POP (2) indexed by the *relaxation order* $d \geq d_{\min}$ is defined as the following SDP:

$$(8) \quad \mathbf{P}_d^{\text{mom}} : \begin{cases} f_d^{\text{mom}} := \inf_{\mathbf{y} \in \mathbb{R}^{N_{2d}^n}} & L_{\mathbf{y}}(f) \\ \text{s.t.} & \mathbf{M}_d(\mathbf{y}) \in \mathcal{S}_+^{s(n,d)}, \\ & \mathbf{M}_{d-d_j}(g_j \mathbf{y}) \in \mathcal{S}_+^{s(n,d-d_j)}, \quad j \in \{1, \dots, m\}, \\ & y_0 = 1. \end{cases}$$

The dual formulation of the infinite-dimensional linear program (5) can be obtained by interpreting f_{\min} as the largest possible lower bound of f over K , namely

$$(9) \quad f_{\min} = \sup_{\lambda \in \mathbb{R}} \{ \lambda \mid \forall \mathbf{x} \in K, f(\mathbf{x}) - \lambda \geq 0 \},$$

which is also a linear program. However, the set of nonnegative polynomials over the set K does not admit any known and computationally efficient representations. Thanks to Putinar's representation theorem [26], one can circumvent this difficulty by requiring $f - \lambda$ to admit a specific weighted SOS representation, namely $f - \lambda = \sum_{j=0}^m \sigma_j g_j$, with each σ_j being an SOS polynomial. The latter condition can also be verified via SDP, yielding the dual formulation of (8), and is called the *SOS relaxation* of order $d \geq d_{\min}$:

$$(10) \quad \mathbf{P}_d^{\text{sos}} : \begin{cases} f_d^{\text{sos}} := \sup_{\lambda \in \mathbb{R}, \mathbf{G}_j} & \lambda \\ \text{s.t.} & f - \lambda = \mathbf{v}_d^\top \mathbf{G} \mathbf{v}_d + \sum_{j=1}^m \mathbf{v}_{d-d_j}^\top \mathbf{G}_j \mathbf{v}_{d-d_j} g_j, \\ & \mathbf{G} \in \mathcal{S}_+^{s(n,d)}, \\ & \mathbf{G}_j \in \mathcal{S}_+^{s(n,d-d_j)}, \quad j \in \{1, \dots, m\}. \end{cases}$$

The sequences of SDP programs (8) and (10) are called the *moment hierarchy* and the *SOS hierarchy*, respectively. While (8) is a *relaxation* of (5), (10) is the corresponding *reinforcement* (or *strengthening*) of the dual (9) of (5). The following assumption, slightly stronger than compactness, and automatically satisfied when K involves one or several ball (in)equality constraints, ensures convergence of the Moment-SOS hierarchy.

Assumption 2.1. *There exists $N > 0$ such that $N - \|\mathbf{x}\|_2^2 = \sum_{j=0}^m \sigma_j g_j$, where each σ_j is an SOS polynomial.*

Theorem 2.2 ([12]). *Under Assumption 2.1, the hierarchies of primal-dual Moment-SOS relaxations (8)-(10) provide non-decreasing sequences of lower bounds converging to f_{\min} .*

For the primal-dual pair (8)-(10), the presence of ball constraints also ensures zero duality gap [8]. Namely, we have $f_d^{\text{sos}} = f_d^{\text{mom}}$ and we can simply write f_d to represent the optimal value of the Moment-SOS hierarchy of order d . In many practical cases, however, we are interested in the convergence of the hierarchy in finitely many steps. Stated differently, we would like the relaxation of order d to be *exact*, meaning that $f_d = f_{\min}$ for some finite, and preferably small, d . Sufficient conditions for this to happen are given by the following theorem:

Theorem 2.3 (Theorem 1.6, [2]). *Consider the hierarchy of moment relaxations defined in (8). If for some $d \geq d_{\min}$ there exists $d' \in \{d_{\min}, \dots, d\}$ such that the SDP problem $\mathbf{P}_d^{\text{mom}}$ has an optimal solution $\mathbf{y}^* \in \mathbb{R}^{\mathbb{N}_{2d}^n}$ which satisfies*

$$(11) \quad \text{rank } \mathbf{M}_{d'}(\mathbf{y}^*) = \text{rank } \mathbf{M}_{d'-d_{\min}}(\mathbf{y}^*),$$

then $f_d = f_{\min}$. Moreover, the infinite-dimensional linear program from (2.1) has an optimal solution $\mu^ \in \mathcal{M}_+(K)$, finitely supported on $r := \text{rank } \mathbf{M}_d(\mathbf{y}^*)$ global minimizers of f on K .*

If the rank condition (11) from Theorem 2.3 is satisfied, then one can extract (some) global minimizers of the initial POP thanks to a numerical linear algebra procedure [7].

Example 2.4. *Let $n = 2$ and consider the following quadratic and nonconvex POP:*

$$(12) \quad \mathbf{P} : \begin{cases} \min_{\mathbf{x} \in K} & f(\mathbf{x}) := -(x_1 - 1)^2 - (x_1 - x_2)^2 - (x_2 - 3)^2, \\ \text{s.t.} & K := \{\mathbf{x} \in \mathbb{R}^2 \mid g_j(\mathbf{x}) \geq 0, j \in \{1, \dots, 4\}\}, \text{ where} \\ & g_1(\mathbf{x}) := 1 - (x_1 - 1)^2, \quad g_2(\mathbf{x}) := 1 - (x_1 - x_2)^2, \\ & g_3(\mathbf{x}) := 1 - (x_2 - 3)^2, \quad g_4(\mathbf{x}) := x_1 - 0.3x_2^2. \end{cases}$$

The first-order moment relaxation of this POP involves the pseudo-moment matrix of size 3 and four linear localizing constraints. Then, $\mathbf{y}_1^ = (1.0, 1.6562, 2.0833, 3.3124, 3.4061, 4.4997) \in \mathbb{R}^{\mathbb{N}_2^2}$*

is the optimal pseudo-moment sequence satisfying $L_{\mathbf{y}_1^*}(f) = f_1 \simeq -3$, and the corresponding first-order pseudo-moment matrix, whose numerical rank is 3, is given by:

$$(13) \quad \mathbf{M}_1(\mathbf{y}_1^*) = \begin{bmatrix} 1.0000 & 1.6562 & 2.0833 \\ 1.6562 & 3.3124 & 3.4061 \\ 2.0833 & 3.4061 & 4.4997 \end{bmatrix}$$

Furthermore, after solving the second-order moment relaxation, which involves a pseudo-moment matrix of size 6 and four localizing matrices of size 3, we eventually obtain the optimal pseudo-moment sequence $\mathbf{y}_2^* = (1, 2, 2, 4, 4, 8, 8, 8, 8, 16, 16, 16, 16, 16) \in \mathbb{R}^{\mathbb{N}_4^2}$ such that $\text{rank } \mathbf{M}_2(\mathbf{y}_2^*) = \text{rank } \mathbf{M}_1(\mathbf{y}_2^*) = 1$, implying that \mathbf{y}_2^* is actually the moment sequence of the Dirac measure concentrated at a global minimizer $\mathbf{x}^* = (2, 2)$, and $L_{\mathbf{y}_2^*}(f) = f_2 = -2 = f_{\min}$.

In [22], it has been proven that the condition from (11), called *flatness condition*, holds generically. However, for many high-dimensional problems, solving higher order relaxations is either too costly or even impossible, since the size of the involved SDP matrices increases rapidly. Indeed at a fixed order d , the corresponding moment relaxation involves a matrix of size $s(n, d) = \binom{n+d}{n} = \mathcal{O}(n^d)$ when $n \rightarrow \infty$. That is why we propose to exploit Christoffel-Darboux kernels to strengthen the relaxation bounds at order d .

2.2. Christoffel-Darboux kernels. The Christoffel-Darboux kernel (CDK) is a well-known and valuable tool in the domain of approximation theory and orthogonal polynomials. Recently, empirical versions of this kernel have emerged, making it quite useful for solving various tasks in the domain of data analysis. Namely, Christoffel-Darboux kernel provides a numerical framework for estimating the support of an unknown measure given only a finite number of its moments. For an in-depth discussion of the Christoffel-Darboux kernels, their properties, and historical developments, see [21, 29, 10, 15].

Let $\mu \in \mathcal{M}_+(\Omega)$, with $\Omega \subset \mathbb{R}^n$ compact with non-empty interior. We highlight that Ω does not necessarily have to represent a feasible set of some POP. The moment matrix of order $d \in \mathbb{N}^*$ associated to μ is given by

$$(14) \quad \mathbf{M}_d(\mu) := \int_{\mathbb{R}^n} \mathbf{v}_d(\mathbf{x})\mathbf{v}_d(\mathbf{x})^\top d\mu(\mathbf{x}) \in \mathcal{S}_+^{s(n,d)},$$

where the integral should be understood component-wise. Such measure μ induces a bilinear form on $\mathbb{R}_d[\mathbf{x}]$, namely, $\langle p, q \rangle_\mu = \int_\Omega p(\mathbf{x})q(\mathbf{x}) d\mu(\mathbf{x})$, for any $p, q \in \mathbb{R}_d[\mathbf{x}]$. If, in addition, $\langle \cdot, \cdot \rangle_\mu$ defines a scalar product then the finite-dimensional space $(\mathbb{R}_d[\mathbf{x}], \langle \cdot, \cdot \rangle_\mu)$ is as a Reproducing Kernel Hilbert space [3]. Its associated kernel is called the *Christoffel-Darboux kernel* (CDK), and it is defined for every $d \in \mathbb{N}^*$ as

$$K_d^\mu : \mathbb{R}^n \times \mathbb{R}^n \ni (\mathbf{x}, \mathbf{y}) \mapsto K_d^\mu(\mathbf{x}, \mathbf{y}) := \sum_{\alpha \in \mathbb{N}_d^n} p_\alpha(\mathbf{x})p_\alpha(\mathbf{y}) \in \mathbb{R},$$

where $(p_\alpha)_{\alpha \in \mathbb{N}_d^n}$ is a family of polynomials that are orthonormal with respect to $\langle \cdot, \cdot \rangle_\mu$. Moreover, whenever $\langle \cdot, \cdot \rangle_\mu$ defines a valid scalar product, or stated equivalently, whenever the moment matrix $\mathbf{M}_d(\mu)$ is invertible, it is possible to show [29] that

$$(15) \quad K_d^\mu(\mathbf{x}, \mathbf{y}) = \mathbf{v}_d(\mathbf{x})^\top \mathbf{M}_d(\mu)^{-1} \mathbf{v}_d(\mathbf{y}), \quad \mathbf{x}, \mathbf{y} \in \mathbb{R}^n.$$

In this case, we can also define the *Christoffel polynomial* Λ_d^μ to be the diagonal of the CDK:

$$(16) \quad \Lambda_d^\mu : \mathbb{R}^d \ni \mathbf{x} \mapsto \Lambda_d^\mu(\mathbf{x}) := K_d^\mu(\mathbf{x}, \mathbf{x}) \in \mathbb{R}_+.$$

By construction, $\Lambda_d^\mu = \sum_{\alpha \in \mathbb{N}_d^n} p_\alpha^2$ is an SOS polynomial of degree $2d$.

Remark 2.5. Notice that the Christoffel-Darboux kernel and, therefore, the Christoffel polynomial itself, only depend on the finite sequence $\mathbf{y} \in \mathbb{R}^{\mathbb{N}_{2d}}$ of moments of μ . Thus, we can interchangeably write Λ_d^μ or $\Lambda_d^\mathbf{y}$, K_d^μ or $K_d^\mathbf{y}$, and $\mathbf{M}_d(\mu)$ or $\mathbf{M}_d(\mathbf{y})$.

One of the most remarkable features of the Christoffel polynomials $(\Lambda_d^\mu)_{d \in \mathbb{N}}$ is their ability to identify the support of the underlying measure μ . Indeed, as explained in [11, Section 4.3, p. 50–51], when increasing the degree d , one may observe the following important dichotomy:

- $\forall \mathbf{x} \in \text{supp}(\mu)$, $\Lambda_d^\mu(\mathbf{x})$ grows at most polynomially, when we let $d \rightarrow +\infty$.
- $\forall \mathbf{x} \notin \text{supp}(\mu)$, $\Lambda_d^\mu(\mathbf{x})$ grows at least exponentially, when we let $d \rightarrow +\infty$.

Then, $\text{supp}(\mu)$ can be approximated via appropriately chosen sublevel sets of the form:

$$(17) \quad S_d(\mu, \gamma) := \{\mathbf{x} \in \mathbb{R}^n \mid \Lambda_d^\mu(\mathbf{x}) \leq \gamma\}.$$

To illustrate this phenomenon, let μ be the uniform measure over the unit square $[0, 1]^2$.

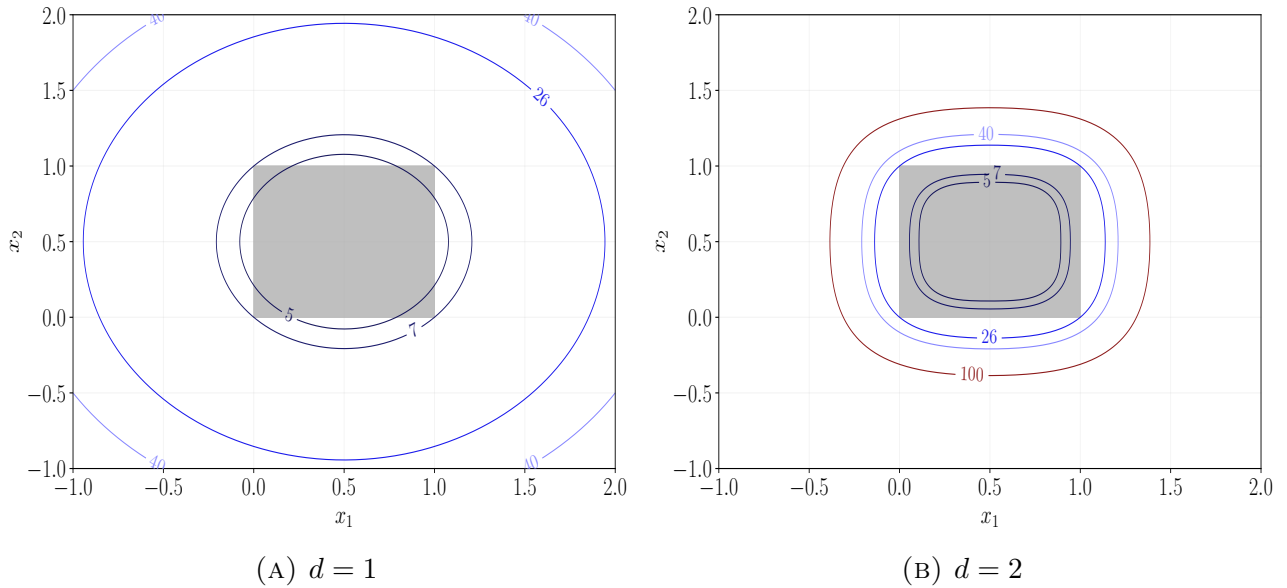


FIGURE 1. Sublevel sets of the Christoffel polynomials associated with the uniform measure over the unit square, i.e., $d\mu(\mathbf{x}) = \mathbb{1}_{[0,1]^2}(\mathbf{x})d\mathbf{x}$. The figure depicts $S_1(\mu, \gamma)$ (left) and $S_2(\mu, \gamma)$ (right) for $\gamma \in \{5, 7, 26, 40, 100\}$.

As displayed in Figure 1, the sublevel sets $S_2(\mu, \gamma)$ constructed using quartic Christoffel polynomials, provide better approximation of the unit square. Furthermore, the exponential growth of $\Lambda_d^\mu(\mathbf{x})$ for points outside of the unit square can be illustrated by, for example, considering the point $\mathbf{x} = (0, 1.25)$, which belongs to $S_1(\mu, 26)$ but does not even belong to $S_2(\mu, 100)$.

3. STRENGTHENING RELAXATION BOUNDS

When solving any POP instance, quite often, the main goal is to recover the optimal measure μ^* , which is finitely supported on the minimizers of f , as described in Theorem 2.3. However, for difficult POPs, the relaxation bound obtained at the step d of the hierarchy is usually not exact, i.e., $f_d < f_{\min}$. Moreover, elevated computational costs can prevent from achieving convergence by computing higher order bounds such as f_{d+1} or f_{d+2} , for example.

In this section, we present two heuristic methods that leverage the information available at order d of the hierarchy. More precisely, these methods aim to construct a modified POP and solve its relaxation at the same order d . Since this modified POP restricts the feasible set, this approach yields tighter bounds. Namely, we will set the new feasible set to be

$$(18) \quad \tilde{K} := K \cap S_d(\mathbf{y}^*, \gamma) = K \cap \left\{ \mathbf{x} \in \mathbb{R}^n \mid \gamma - \Lambda_d^{\mathbf{y}^*}(\mathbf{x}) \geq 0 \right\},$$

where \mathbf{y}^* is the optimal solution of the initial relaxation at order d , and $\gamma > 0$ is the parameter to be tuned. In what follows, we argue that this approach can help obtaining a tighter lower bound \tilde{f}_d such that $f_d \leq \tilde{f}_d \leq f_{\min}$, and potentially enable the extraction of minimizers, *even at step d of the hierarchy*. Before delving into a detailed description of our method, we first outline some of the general challenges associated with it.

Firstly, the pseudo-moment matrix $\mathbf{M}_d(\mathbf{y}^*)$ may only be positive semidefinite, in which case computing $\Lambda_d^{\mathbf{y}^*}$ as described in (16) would introduce a significant amount of numerical instability and inaccuracy. We attempt to mitigate these problems by computing the Christoffel polynomials in a slightly different manner. Notice that we can always write

$$(19) \quad \mathbf{M}_d(\mathbf{y}^*) = \mathbf{P}\mathbf{E}\mathbf{P}^\top,$$

where \mathbf{P} is an orthonormal matrix of size $s(n, d)$ whose columns are denoted by \mathbf{p}_i , $i \in \{1, \dots, s(n, d)\}$, and $\mathbf{E} \in \mathcal{S}_+^{s(n, d)}$ is the diagonal matrix containing the eigenvalues $e_1 \geq \dots \geq e_i \geq \dots \geq e_{s(n, d)} \geq 0$ of $\mathbf{M}_d(\mathbf{y}^*)$. Interpreting the eigenvectors \mathbf{p}_i as coefficients of polynomials $p_i \in \mathbb{R}_d[\mathbf{x}]$ yields the *Tikhonov regularization* of the Christoffel polynomial of order d :

$$(20) \quad \tilde{\Lambda}_d^{\mathbf{y}^*} := \sum_{i=1}^{s(n, d)} \frac{p_i^2}{e_i + \beta},$$

where $\beta > 0$ is a small regularization parameter. A measure-theoretic interpretation of this regularization can be found in [20]. For instance, if we suppose that $\mathbf{M}_d(\mathbf{y}^*)$ is expressed in the basis of polynomials $(q_\alpha)_\alpha$ that are orthonormal w.r.t. the Lebesgue measure λ on K , and if \mathbf{y}_λ denotes the moment sequence of λ , then $\tilde{\Lambda}_d^{\mathbf{y}^*} = \Lambda_d^{\mathbf{y}^* + \beta \mathbf{y}_\lambda}$, where

$$(21) \quad L_{\mathbf{y}^* + \beta \mathbf{y}_\lambda}(p) = L_{\mathbf{y}^*}(p) + \beta \int_K p(\mathbf{x}) d\lambda(\mathbf{x}), \quad \forall p \in \mathbb{R}_{2d}[\mathbf{x}],$$

$$(22) \quad \mathbf{M}_d(\mathbf{y}^* + \beta \mathbf{y}_\lambda)(\boldsymbol{\alpha}, \boldsymbol{\gamma}) = L_{\mathbf{y}^*}(q_\alpha q_\gamma) + \beta \mathbb{1}_{\boldsymbol{\alpha}=\boldsymbol{\gamma}}, \quad \forall \boldsymbol{\alpha}, \boldsymbol{\gamma} \in \mathbb{N}_d^n.$$

If we denote by $r \in \mathbb{N}$ the number of zero eigenvalues, or, stated differently, the dimension of the kernel of the pseudo-moment matrix $\mathbf{M}_d(\mathbf{y}^*)$, then the sublevel sets associated to $\tilde{\Lambda}_d^{\mathbf{y}^*}$ that we will use for strengthening the relaxations can be written in the following way:

$$(23) \quad \tilde{S}_d(\mathbf{y}^*, \gamma) := \left\{ \mathbf{x} \in \mathbb{R}^n \mid \sum_{i=1}^{s(n, d)-r} \frac{p_i^2(\mathbf{x})}{e_i + \beta} \leq \gamma, p_j^2(\mathbf{x}) \leq \beta, s(n, d) - r + 1 \leq j \leq s(n, d) \right\}.$$

The rationale behind the expression in (23) is as follows: if $\mathbf{x} \in \mathbb{R}^n$ is such that there exists $j \in \{s(n, d) - r + 1, \dots, s(n, d)\}$ for which $p_j^2(\mathbf{x}) > 0$, then division by the associated eigenvalue $e_j + \beta$ would result in a very large positive term. Consequently, such an \mathbf{x} would not belong to the γ -sublevel set for any reasonably large γ . Thus, it is reasonable to believe that the minimizers of f should be contained in the neighborhood of the algebraic variety $\{\mathbf{x} \in \mathbb{R}^n \mid p_j^2(\mathbf{x}) = 0, j \in \{s(n, d) - r + 1, \dots, s(n, d)\}\}$. Moreover, the sum involving polynomials that are not in the kernel of the pseudo-moment matrix should help us identify a more precise location within this variety where the minimizers could lie.

Secondly, the challenge lies in appropriately selecting the threshold $\gamma > 0$. If γ is too small, the resulting feasible set may shrink excessively. On the other hand, if γ is too large, the relaxation may remain too loose, failing to improve the bound in a meaningful way. To illustrate this more effectively, let us revisit Example 2.4.

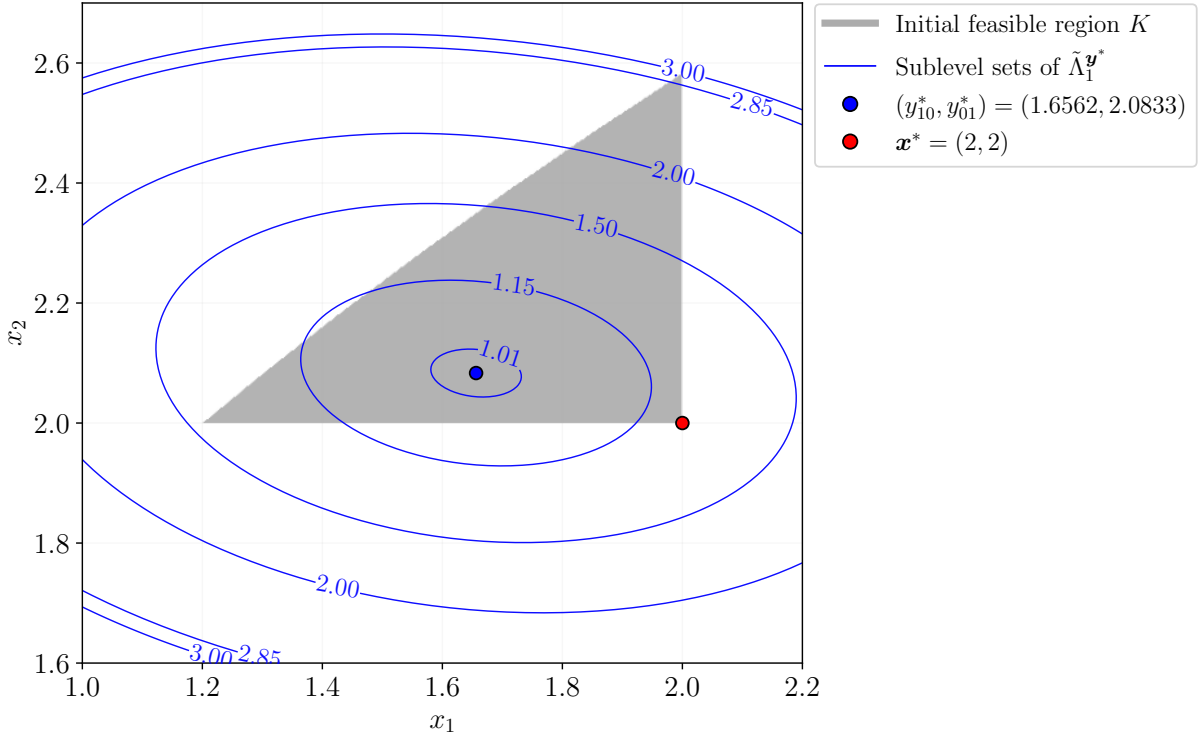


FIGURE 2. Depicting sublevel sets $\tilde{S}_1(\mathbf{y}^*, \gamma)$ associated to the POP from Example 2.4, where $\gamma \in \{1.01, 1.15, 1.50, 2.00, 2.85, 3.0\}$. The red point is the true minimizer of f , and the blue point corresponds to the pseudo-moments of order one extracted from the optimal solution \mathbf{y}^* of the first-order moment relaxation.

As depicted in Figure 2, different sublevel sets induce different restrictions of the initial feasible set K . For example, with $\gamma = 1.50$, the upper part of K is eliminated, resulting in a *valid and improved* lower bound \tilde{f}_1 such that $f_{\min} = -2 > \tilde{f}_1 = -2.3131 > f_1 = -3$. On the other hand, any γ that is too small could overly restrict K , and eventually make the true minimizer of f unfeasible. For instance, if $\gamma = 1.15$, we obtain an *invalid* (upper) bound $\tilde{f}_1 = -1.8577 > f_{\min}$. To summarize, level sets of the Christoffel polynomial of order d give us valuable information about the location of the true minimizers of f . To leverage this information, efficient control of the parameter γ is essential. The following subsections present two heuristic methods to balance lower bound tightness with the risk of obtaining an upper bound.

3.1. Iterative approach - H1. The first heuristic method we propose, called **H1**, is aimed at progressively reducing the feasible set until a more satisfactory lower bound is obtained. This approach relies on re-executing relaxations of order d , which is often more efficient than increasing the relaxation order in the hierarchy, particularly if the number of re-executions or iterations remains relatively small. At each iteration $k \geq 1$, the γ_k -sublevel set is selected in such a way that the previously optimal pseudo-moment sequence $\mathbf{y}_{(k-1)}^* \in \mathbb{R}^{\mathbb{N}_{2d}^n}$ becomes infeasible for the modified POP, forcing the lower bound to improve. Choosing the threshold γ_k which ensures this behavior is based on the following proposition:

Proposition 3.1. *Let $d \in \mathbb{N}^*$ and $\mathbf{y}^* \in \mathbb{R}^{\mathbb{N}_{2d}^n}$ be an optimal solution of the moment relaxation of order d . Then,*

$$(24) \quad L_{\mathbf{y}^*} \left(\tilde{\Lambda}_d^{\mathbf{y}^*} \right) = \sum_{i=1}^{s(n,d)-r} \frac{e_i}{e_i + \beta} \quad (\approx \text{rank } \mathbf{M}_d(\mathbf{y}^*) \text{ when } \beta \text{ is small}).$$

Proof. From (19) and (20) one has

$$\begin{aligned}
(25) \quad L_{\mathbf{y}^*} \left(\tilde{\Lambda}_d^{\mathbf{y}^*} \right) &= L_{\mathbf{y}^*} \left(\sum_{i=1}^{s(n,d)} \frac{p_i^2}{e_i + \beta} \right) = \sum_{i=1}^{s(n,d)} \frac{1}{e_i + \beta} L_{\mathbf{y}^*} (p_i^2) \\
&= \sum_{i=1}^{s(n,d)} \frac{1}{e_i + \beta} \mathbf{p}_i^\top \mathbf{M}_d(\mathbf{y}^*) \mathbf{p}_i = \sum_{i=1}^{s(n,d)} \frac{1}{e_i + \beta} e_i \mathbb{1}_{\mathbf{p}_i \notin \ker \mathbf{M}_d(\mathbf{y}^*)}.
\end{aligned}$$

As the dimension of the kernel of the pseudo-moment matrix $\mathbf{M}_d(\mathbf{y}^*)$ is $r \in \mathbb{N}^*$, one obtains

$$(26) \quad L_{\mathbf{y}^*} \left(\tilde{\Lambda}_d^{\mathbf{y}^*} \right) = \sum_{i=1}^{s(n,d)-r} \frac{e_i}{e_i + \beta},$$

and therefore $L_{\mathbf{y}^*} \left(\tilde{\Lambda}_d^{\mathbf{y}^*} \right) \approx \text{rank}(\mathbf{M}(\mathbf{y}^*))$ when β is small, which concludes the proof. \square

Thus, by choosing $\gamma \geq L_{\mathbf{y}^*}(\tilde{\Lambda}_d^{\mathbf{y}^*})$, minimizing f over $\tilde{K} = K \cap \tilde{S}_d(\mathbf{y}^*, \gamma)$ yields little improvement, as the existing optimal solution \mathbf{y}^* remains feasible. Instead, using the penalized threshold $\gamma = (1 - \varepsilon)L_{\mathbf{y}^*}(\tilde{\Lambda}_d^{\mathbf{y}^*})$ with $\varepsilon \in (0, 1)$ excludes \mathbf{y}^* from the feasible set, improving the lower bound. This process is repeated until a maximum number of iterations is reached or the bound improvement is deemed satisfactory. The true optimal value f_{\min} being unknown, we assess the tightness of the new lower bound \tilde{f}_d by computing the (*relative*) *optimality gap*:

$$(27) \quad \Delta(f(\bar{\mathbf{x}}), \tilde{f}_d) := \left(\frac{|f(\bar{\mathbf{x}}) - \tilde{f}_d|}{|f(\bar{\mathbf{x}})|} \mathbb{1}_{f(\bar{\mathbf{x}}) \neq 0} + |f(\bar{\mathbf{x}}) - \tilde{f}_d| \mathbb{1}_{f(\bar{\mathbf{x}}) = 0} \right) \times 100\%,$$

where $f(\bar{\mathbf{x}})$ is a valid upper bound of f_{\min} obtained by evaluating f at a given locally optimal solution $\bar{\mathbf{x}} \in \mathbb{R}^n$. The steps of this iterative approach **H1** are outlined in Algorithm 1.

Algorithm 1 Implementing **H1**

Input: Relaxation order d , gap tolerance $\delta > 0$, maximum number of iterations N , and a penalization factor $\varepsilon \in (0, 1)$.

Initialize: $k = 0$

(1) Initialize the feasible set $\tilde{K}_k = K$.

(2) Solve the moment relaxation of order d . Recover its optimal solution \mathbf{y}_k^* , relaxation bound $\tilde{f}_{d,k} = f_d$, and a local solution $\bar{\mathbf{x}}_k$ yielding an upper bound $\text{ub}_k = f(\bar{\mathbf{x}}_k)$.

(3) Initialize the relative gap $\Delta_k = \Delta \left(f(\bar{\mathbf{x}}_k), \tilde{f}_{d,k} \right)$.

While $k < N$

(4) **If** $\tilde{f}_{d,k} > \text{ub}_k$ **or** $\Delta_k \leq \delta$
 – **Break.**

(5) Compute the Christoffel polynomial $\tilde{\Lambda}_d^{\mathbf{y}_k^*}$ and set $\gamma_k = L_{\mathbf{y}_k^*} \left(\tilde{\Lambda}_d^{\mathbf{y}_k^*} \right)$.

(6) Modify the feasible set via $\tilde{K}_{k+1} = \tilde{K}_k \cap \tilde{S}_d(\mathbf{y}_k^*, (1 - \varepsilon)\gamma_k)$, and solve the moment relaxation of order d . Recover the new relaxation bound $\tilde{f}_{d,k+1}$, the new optimal solution \mathbf{y}_{k+1}^* , and the new locally optimal solution $\bar{\mathbf{x}}_{k+1}$.

(7) Set $\text{ub}_{k+1} = \min_{i \in \{0, k+1\}} \{f(\bar{\mathbf{x}}_{i+1})\}$ and re-evaluate the gap $\Delta_{k+1} = \Delta \left(\text{ub}_{k+1}, \tilde{f}_{d,k+1} \right)$.

(8) Update the iteration count $k = k + 1$.

Output: Sequence of bounds $\left(\tilde{f}_{d,k} \right)_{k \geq 1}$ satisfying $\tilde{f}_{d,k+1} \geq \tilde{f}_{d,k} \geq f_d$.

We emphasize that there are no guarantees that Algorithm 1 will produce a sequence $(\tilde{f}_{d,k})_{k \geq 1}$ such that its last element is a valid lower bound of f_{\min} . However, our experimental results presented in Section 4 suggest that such *non-desirable* occurrences are relatively rare.

Remark 3.1. Notice from step (6) of Algorithm 1 that, at each iteration, all previously added sublevel constraints are retained. This ensures that the feasible set of POP is progressively restricted, and, in turn, that no previously excluded optimal pseudo-moment sequences re-enter the feasible set of moment relaxations.

The behavior of Algorithm 1 is illustrated on Example 2.4, with results shown in Figure 3.

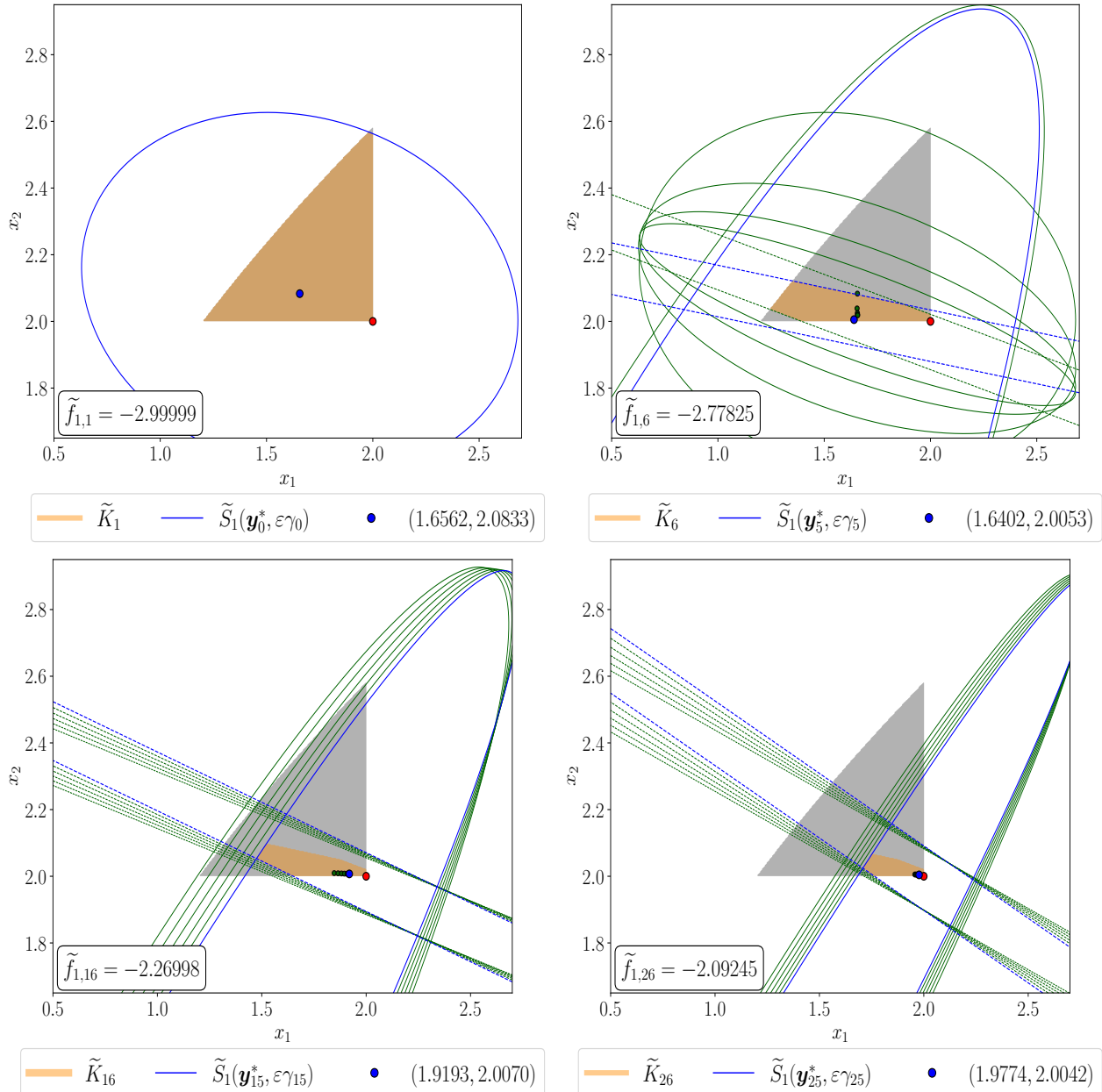


FIGURE 3. Different iterations $k \in \{0, 5, 15, 25\}$ of Algorithm 1, with $\varepsilon = 0.95$.

Let us provide a detailed description of the Figure 3. The red point $\mathbf{x}^* = (2, 2)$ is the global minimizer. Green curves correspond to the level sets of Christoffel polynomials from the preceding 5 iterations, while blue lines indicate the level sets for the current iteration. If the 3×3 pseudo-moment matrix is of full rank, only solid lines are present. In contrast, dashed lines

represent the contribution of polynomials that belong to the kernel of the corresponding pseudo-moment matrix. Green points represent the pseudo-moments of order one associated with the 5 preceding iterations, whereas the blue point depicts the pseudo-moments of order one for the current iteration. Figure 3 illustrates how the successively constructed Christoffel polynomials contribute to improving the relaxation bounds from $\tilde{f}_{1,1} = -2.99999$ to $\tilde{f}_{1,26} = -2.09245$. This improvement is achieved through informed incremental restrictions of the feasible set \tilde{K}_k , depicted in orange. Furthermore, we observe a clear convergence of the pseudo-moments of order one, $(y_{k,10}^*, y_{k,01}^*)_{0 \leq k \leq 25}$, towards the moments of order one associated with the Dirac measure at the point $(2, 2)$. Finally, note the reduction in the areas of sublevel sets $\tilde{S}_1(\mathbf{y}_k^*, 0.95\gamma_k)_{0 \leq k \leq 25}$, indicating a decrease in uncertainty about the minimizer's location.

3.2. Local-solution-based approach - H2. Unlike the previous heuristic, where the reduction of the feasible set was entirely guided by the information extracted from the relaxation itself, our second heuristic, named **H2**, explicitly leverages some available solution $\bar{\mathbf{x}} \in \mathbb{R}^n$ which is *locally optimal*, to determine the shape of the new feasible set. This procedure involves constructing *univariate* or *marginal* Christoffel polynomials to assess the quality of the given local solution and to selectively add constraints to the initial POP, thereby strengthening the lower bound of the moment relaxations.

Let $i \in \{1, \dots, n\}$. We define $\mathbb{N}_d^{n[i]} := \{\boldsymbol{\alpha} = (\alpha_1, \dots, \alpha_i, \dots, \alpha_n) \in \mathbb{N}_d^n \mid \alpha_j = 0, \forall j \neq i\}$. Then, from any sequence $\mathbf{y} \in \mathbb{R}^{\mathbb{N}_{2d}^n}$ we can extract the corresponding subsequence $\mathbf{y}_{[i]} \in \mathbb{R}^{\mathbb{N}_{2d}^{n[i]}}$ representing only the pseudo-moments related to the variable x_i . Consequently, $\mathbf{M}_d(\mathbf{y}_{[i]})$ denotes the *marginal* pseudo-moment matrix of size $(d+1)$, associated to the variable x_i . For example, if $n = 2, d = 1$ and $i = 2$, we obtain

$$(28) \quad \mathbf{y}_{[2]} = (1, y_{01}, y_{02}) \quad \text{and} \quad \mathbf{M}_1(\mathbf{y}_{[2]}) = \begin{bmatrix} 1 & y_{01} \\ y_{01} & y_{02} \end{bmatrix}.$$

Furthermore, we define the *marginal* Christoffel polynomial associated to the variable x_i to be

$$(29) \quad \tilde{\Lambda}_d^{\mathbf{y}_{[i]}} : \mathbb{R} \ni x_i \mapsto \sum_{j=1}^{d+1} \frac{p_j^2(x_i)}{e_j + \beta} \in \mathbb{R}_+,$$

where $\beta > 0$, and the orthonormal polynomials $(p_j)_{j \leq d+1}$ and eigenvalues $(e_j)_{j \leq d+1}$ are obtained from the spectral decomposition of $\mathbf{M}_d(\mathbf{y}_{[i]})$. Analogously, associated γ -sublevel sets are denoted by $\tilde{S}_d(\mathbf{y}_{[i]}, \gamma)$.

Let us recall that $\mathbf{y}^* \in \mathbb{R}^{\mathbb{N}_{2d}^n}$ denotes the optimal pseudo-moment sequence of the moment relaxation at order d . Then, **H2** relies on constructing n sublevel constraints, one for each coordinate x_i . These constraints are derived from the sublevel sets of marginal Christoffel polynomials, with the sublevel threshold $\gamma_i > 0$ being defined as the evaluation of the marginal Christoffel polynomial $\tilde{\Lambda}_1^{\mathbf{y}_{[i]}^*}$ at the corresponding coordinate of the local solution $\bar{\mathbf{x}} \in \mathbb{R}^n$, namely

$$(30) \quad \gamma_i := \tilde{\Lambda}_1^{\mathbf{y}_{[i]}^*}(\bar{x}_i), \quad i \in \{1, \dots, n\}.$$

The effectiveness of this approach depends critically on the quality of the local solution. Bad local solutions can cause the Christoffel polynomials to fail in capturing the correct information. We can partially address these risks by carefully selecting the sublevel sets $\tilde{S}_1(\mathbf{y}_{[i]}, \gamma_i)$ to be intersected with the initial feasible set K . To do so, we leverage the following property of the Christoffel polynomials:

Proposition 3.2. *Let $\mathbf{y}^* \in \mathbb{R}^{\mathbb{N}_{2a}^n}$ be such that matrix $\mathbf{M}_1(\mathbf{y}^*) \in \mathcal{S}_+^{n+1}$ is invertible. Define $\hat{\mathbf{x}} := (L_{\mathbf{y}^*}(x_1), \dots, L_{\mathbf{y}^*}(x_n)) \in \mathbb{R}^n$. Then, the Christoffel polynomial $\Lambda_1^{\mathbf{y}^*}$ verifies*

$$(31) \quad \min_{\mathbf{x} \in \mathbb{R}^n} \Lambda_1^{\mathbf{y}^*}(\mathbf{x}) = 1 = \Lambda_1^{\mathbf{y}^*}(\hat{\mathbf{x}}).$$

Proof. Notice that there exists some $\mathbf{Y}^* \in \mathcal{S}_+^n$ such that $\mathbf{M}_1(\mathbf{y}^*) = \begin{bmatrix} 1 & \hat{\mathbf{x}}^\top \\ \hat{\mathbf{x}} & \mathbf{Y}^* \end{bmatrix}$. Since $\mathbf{M}_1(\mathbf{y}^*)$ is invertible, using the Schur's complement lemma, we deduce that \mathbf{Y}^* is also invertible, and that

$$(32) \quad \mathbf{M}_1(\mathbf{y}^*)^{-1} = \frac{1}{c} \begin{bmatrix} 1 & -\hat{\mathbf{x}}^\top \mathbf{Y}^{*-1} \\ -\mathbf{Y}^{*-1} \hat{\mathbf{x}} & \mathbf{Y}^{*-1} \hat{\mathbf{x}} \hat{\mathbf{x}}^\top \mathbf{Y}^{*-1} + c \mathbf{Y}^{*-1} \end{bmatrix},$$

with $c = 1 - \hat{\mathbf{x}}^\top \mathbf{Y}^{*-1} \hat{\mathbf{x}} > 0$. Then, for any $\mathbf{x} \in \mathbb{R}^n$, the following holds:

$$(33) \quad \begin{aligned} \Lambda_1^{\mathbf{y}^*}(\mathbf{x}) &= \mathbf{v}_1(\mathbf{x})^\top \mathbf{M}_1(\mathbf{y}^*)^{-1} \mathbf{v}_1(\mathbf{x}) \\ &= c^{-1} - 2c^{-1} \mathbf{x}^\top \mathbf{Y}^{*-1} \hat{\mathbf{x}} + \mathbf{x}^\top (c^{-1} \mathbf{Y}^{*-1} \hat{\mathbf{x}} \hat{\mathbf{x}}^\top \mathbf{Y}^{*-1} + \mathbf{Y}^{*-1}) \mathbf{x} \\ &= \mathbf{x}^\top \mathbf{Y}^{*-1} \mathbf{x} + c^{-1} (1 - \mathbf{x}^\top \mathbf{Y}^{*-1} \hat{\mathbf{x}})^2. \end{aligned}$$

Invertibility of \mathbf{Y}^* implies that $\Lambda_1^{\mathbf{y}^*}$ is convex. Hence, we can recover its minimizer $\mathbf{x}^* \in \mathbb{R}^n$ by applying the first-order, necessary and sufficient, condition. The gradient of $\Lambda_1^{\mathbf{y}^*}$ is given by:

$$(34) \quad \nabla \Lambda_1^{\mathbf{y}^*}(\mathbf{x}^*) = 2\mathbf{Y}^{*-1} \mathbf{x}^* - 2c^{-1} (1 - \mathbf{x}^{*\top} \mathbf{Y}^{*-1} \hat{\mathbf{x}}) \mathbf{Y}^{*-1} \hat{\mathbf{x}},$$

so that

$$(35) \quad \begin{aligned} \nabla \Lambda_1^{\mathbf{y}^*}(\mathbf{x}^*) = 0 &\implies \mathbf{x}^* = c^{-1} (1 - \mathbf{x}^{*\top} \mathbf{Y}^{*-1} \hat{\mathbf{x}}) \hat{\mathbf{x}} \\ &\implies \mathbf{x}^{*\top} \mathbf{Y}^{*-1} \hat{\mathbf{x}} = c^{-1} \hat{\mathbf{x}}^\top \mathbf{Y}^{*-1} \hat{\mathbf{x}} - c^{-1} \mathbf{x}^{*\top} \mathbf{Y}^{*-1} \hat{\mathbf{x}} \hat{\mathbf{x}}^\top \mathbf{Y}^{*-1} \hat{\mathbf{x}} \\ &\implies \mathbf{x}^{*\top} \mathbf{Y}^{*-1} \hat{\mathbf{x}} = \frac{\hat{\mathbf{x}}^\top \mathbf{Y}^{*-1} \hat{\mathbf{x}}}{c + \hat{\mathbf{x}}^\top \mathbf{Y}^{*-1} \hat{\mathbf{x}}} \\ &\implies (\mathbf{x}^* - \hat{\mathbf{x}})^\top \mathbf{Y}^{*-1} \hat{\mathbf{x}} = 0 \implies \mathbf{x}^* = \hat{\mathbf{x}}. \end{aligned}$$

Finally, notice that $\Lambda_1^{\mathbf{y}^*}(\hat{\mathbf{x}}) = \hat{\mathbf{x}}^\top \mathbf{Y}^{*-1} \hat{\mathbf{x}} + \frac{(1 - \hat{\mathbf{x}}^\top \mathbf{Y}^{*-1} \hat{\mathbf{x}})^2}{1 - \hat{\mathbf{x}}^\top \mathbf{Y}^{*-1} \hat{\mathbf{x}}} = 1$, which concludes the proof. \square

Remark 3.2. *In order to simplify the proof, Proposition 3.2 was stated in terms of $\Lambda_1^{\mathbf{y}^*}$, but analogous conclusions can be derived for the regularized function $\tilde{\Lambda}_1^{\mathbf{y}^*}$. In addition, the result from Proposition 3.2 holds true regardless of whether the vector \mathbf{y}^* can be represented by a measure.*

Based on Proposition 3.2, if there exists some $i \in \{1, \dots, n\}$ such that the threshold γ_i is significantly larger than one, this implies that the coordinate i of the local solution $\bar{\mathbf{x}}$ is substantially far from the relaxation-dependent value $L_{\mathbf{y}^*}(x_i)$. This, in turn, suggests either that the local solution \bar{x}_i deviates significantly from x_i^* , or that the relaxation quality is poor.

Conversely, values of γ_i close to one indicate agreement between the local solver and the relaxation on the potential location of the coordinate i of the true minimizer. In such cases, it appears reasonable to search for the true minimizer within the set

$$(36) \quad \left\{ \mathbf{x} \in \mathbb{R}^n \mid x_i \in \tilde{S}_1(\mathbf{y}_{[i]}^*, \gamma_i) \right\}.$$

Thus, we modify the initial feasible set by intersecting it with the sets described in (36), but only when the threshold γ_i is smaller than a user-defined *filtering parameter* $\tau > 1$. The steps of this local-solution-based strengthening approach **H2** are formalized in the Algorithm 2.

Algorithm 2 Implementing **H2****Input:** Relaxation order d , parameter $\tau > 1$.

- (1) Solve the moment relaxation of order d . Recover its optimal solution \mathbf{y}^* and a local solution $\bar{\mathbf{x}}$.
- (2) Construct the marginal Christoffel polynomials $\tilde{\Lambda}_1^{\mathbf{y}^*[i]}$ and compute the thresholds $\gamma_i = \tilde{\Lambda}_1^{\mathbf{y}^*[i]}(\bar{x}_i)$, for $i \in \{1, \dots, n\}$.
- (3) Modify the feasible set via $\tilde{K} = K \cap \bigcap_{i: \gamma_i \leq \tau} \left\{ \mathbf{x} \in \mathbb{R}^n \mid x_i \in \tilde{S}_1(\mathbf{y}^*[i], \gamma_i) \right\}$, and solve the moment relaxation of order d .

Output: Tightened bound $\tilde{f}_d \geq f_d$.

Notice that it is possible, for instance, for the local solution \bar{x}_i and the corresponding pseudo-moment $L_{\mathbf{y}^*}(x_i)$ to be very close to each other, while both are simultaneously significantly far from the true solution x_i^* . In this case, adding the associated sublevel constraint could result in obtaining an invalid bound. However, for a carefully tuned filtering value τ , the percentage of such cases is quite small, as suggested by our experimental results from Section 4. Finally, let us graphically illustrate the behaviour of Algorithm 2 using Example 2.4.

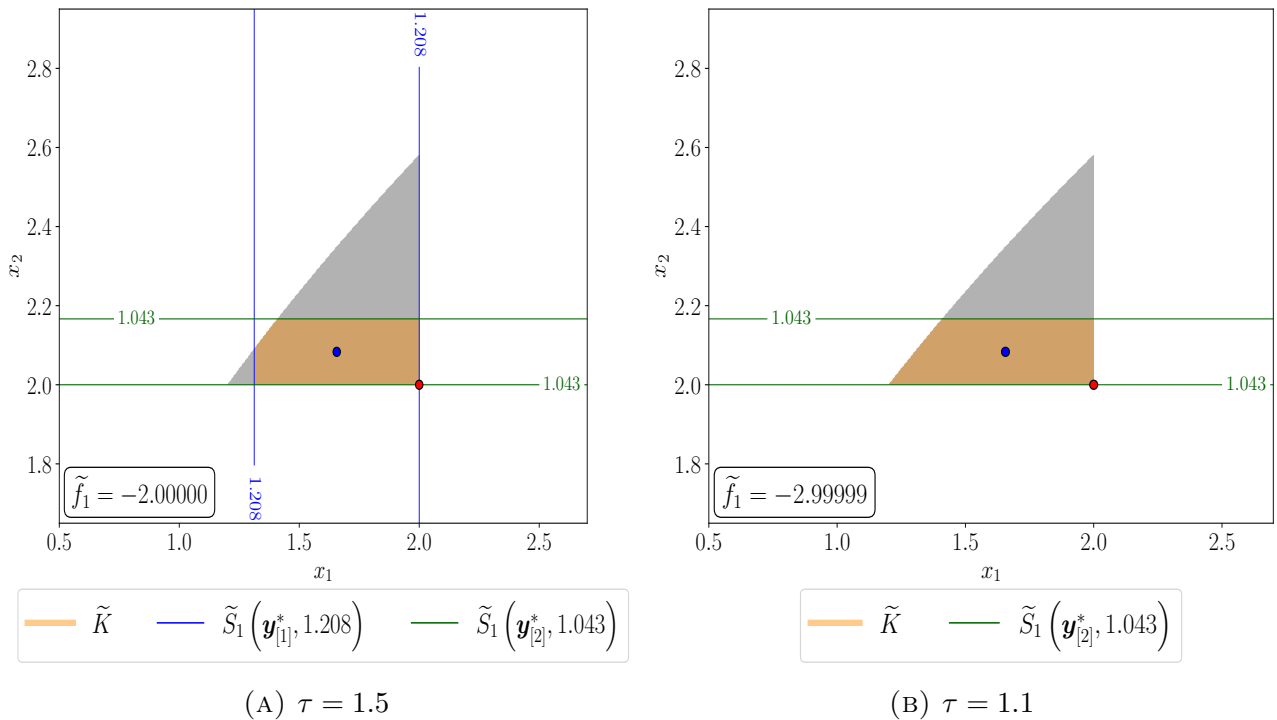


FIGURE 4. Algorithm 2 applied to Example 2.4 for different values of τ . The blue point is $\hat{\mathbf{x}} = (1.6562, 2.0833)$, and the red point corresponds to $\bar{\mathbf{x}} = \mathbf{x}^* = (2, 2)$.

In the case of Example 2.4, the locally optimal solution to which we had access happened to be globally optimal as well. Moreover, given the previously optimal \mathbf{y}^* , setting the filtering parameter to $\tau = 1.5$, for instance, results in both $\tilde{S}_1(\mathbf{y}^*_{[1]}, 1.208)$ and $\tilde{S}_1(\mathbf{y}^*_{[2]}, 1.043)$ being intersected with the initial feasible set, since both γ_1 and γ_2 are smaller than $\tau = 1.5$. Consequently, the new relaxation bound improves significantly, yielding $\tilde{f}_1 = -2$. In contrast, setting $\tau = 1.1$ results in only $\tilde{S}_1(\mathbf{y}^*_{[2]}, 1.043)$ being considered, as the certainty regarding the location of x_1 is not deemed sufficient. This, in turn, leads to a less restrictive modification of the initial feasible set, resulting in no improvement in the bound, i.e., $\tilde{f}_1 = -3$.

4. NUMERICAL EXPERIMENTS

In this section, we present the numerical results of applying our heuristics to different classes of polynomial optimization problems with inexact relaxations of order d .

All experiments were performed on a computer with a 13th Gen Intel Core i7-13620H CPU @ 2.40 GHz, 10 cores, 16 logical processors, and 32GB of RAM. Exact optimal values of all studied optimization problems were computed on one of the CALMIP servers with 2 Intel Xeon Gold 6140 CPUs @ 2.30 GHz, with a total of 72 logical processors (18 cores per socket, 2 threads per core) and a RAM of 600GB. All the studied POP instances were modeled using the Julia library TSSOS [18], and their corresponding Moment-SOS relaxations were solved with Mosek [1]. Locally optimal solutions were obtained using the local solver Ipopt [30]. The numerical implementation of our algorithms, along with the corresponding experimental results, are available in this GitHub repository: [CDK_Bound_Strengthening](#).

4.1. **QCQP over $[0, 1]^n$.** The first part of this section focuses on quadratically constrained quadratic programs (QCQPs) of the following form:

$$(37) \quad \min_{\mathbf{x} \in \mathbb{R}^n} \{ \mathbf{x}^\top \mathbf{Q} \mathbf{x} + \mathbf{x}^\top \mathbf{q} \mid \mathbf{0} \leq \mathbf{x} \leq \mathbf{1} \},$$

where $\mathbf{Q} \in \mathcal{S}^n$ and $\mathbf{q} \in \mathbb{R}^n$. The first-order Moment-SOS relaxation of these problems is not always exact, which provides an interesting benchmark for testing the effectiveness of our heuristics. We consider two classes of input data (\mathbf{Q}, \mathbf{q}) , distinguished by the percentage s of zero entries they contain.

- (1) (\mathbf{Q}, \mathbf{q}) are randomly generated from $\mathcal{N}(0, 1)$, with $s = 0\%$;
- (2) (\mathbf{Q}, \mathbf{q}) are randomly generated from $\mathcal{N}(0, 1)$, with $s = 20\%$.

We create 50 instances of these problems by varying the random seeds, considering two different dimensions: $n = 20$, and $n = 30$. For the moment, we restrict ourselves to medium-size dimensions to ensure access to the true optimal values of the associated POPs, since those true values are required to assess the efficiency of our methods. In scenarios where problems *lack inherent structure* —as is the case here—computing exact optimal values in higher dimensions is neither reasonable nor practical. Table 1 contains explanations of different metrics that were used to assess the performance of our methods.

Notation	Description
$\tilde{f}_1 > f_{\min}$	Number of instances (out of 50) where the method over-restricted the feasible set, leading to an <i>invalid</i> (upper) bound.
Gap (%)	Relative optimality gaps computed before $(\Delta(f_1, f_{\min}))$ and after $(\Delta(\tilde{f}_1, f_{\min}))$ applying the heuristic.
Time (s)	Computational time (in seconds) required for solving the second-order relaxation (f_2) and for computing the heuristic bounds (\tilde{f}_1).
Solved	Number of instances where $\Delta(\tilde{f}_1, f_{\min})$ is below the tolerance $\delta\%$.
k	Number of iterations from the Algorithm 1.

TABLE 1. Summary of column names used in Tables 2, 3, 4 and 5. Columns “Gap (%)”, “Time (s)” and “ k ” represent *averages* over the instances for which a *valid* post-heuristic bound \tilde{f}_1 was obtained.

4.1.1. *Performance of H1.* We start by assessing the performance of **H1**, implemented via Algorithm 1, where we set optimality gap tolerance to be $\delta = 0.5\%$, and a maximum number of iterations $N = 15$. The kernel dimension was determined by counting the number of eigenvalues of the corresponding moment matrices smaller than 10^{-3} . The regularization parameter for computing the Christoffel sublevel sets was set to $\beta = 10^{-5}$.

n	s	ε	$\tilde{f}_1 > f_{\min}$	Gap (%)		Time (s)		Solved	k
				$\Delta(f_1, f_{\min})$	$\Delta(\tilde{f}_1, f_{\min})$	\tilde{f}_1	f_2		
20	0 %	0.01	1	4.853	2.755	0.397	26.256	13	13.80
		0.05	4	4.649	1.687	0.253	26.387	20	8.09
		0.1	2	4.757	1.629	0.221	26.404	16	6.65
		0.15	2	4.757	2.132	0.161	26.404	11	5.02
	20 %	0.01	2	4.668	2.591	0.407	26.659	13	14.10
		0.05	3	4.540	1.256	0.259	26.727	22	8.43
		0.1	4	4.415	1.379	0.195	26.739	20	6.37
		0.15	4	4.304	1.732	0.136	26.733	14	4.28
30	0 %	0.01	0	5.419	3.962	0.869	1206.587	9	14.00
		0.05	4	5.318	2.361	0.728	1211.969	16	10.98
		0.1	5	5.404	2.004	1.007	1209.611	13	10.16
		0.15	6	5.132	1.749	0.829	1208.643	14	7.36
	20 %	0.01	0	6.059	4.784	0.899	1163.134	2	14.84
		0.05	2	5.959	2.927	0.870	1165.358	12	13.04
		0.1	2	5.871	2.300	0.819	1165.310	13	11.94
		0.15	9	5.074	1.790	0.566	1172.107	10	8.41

TABLE 2. Performance of **H1** in dimensions 20 and 30, for different values of the penalization factor ε .

From Table 2, we observe that when ε is small (e.g., $\varepsilon = 0.01$), the method progresses cautiously, requiring on average a larger number of iterations, regardless of the dimension. On the other hand, moderate values of ε (e.g., $\varepsilon = 0.05$ or $\varepsilon = 0.1$) significantly improve optimality gaps while inducing smaller running times. Finally, the feasible set restrictions imposed when $\varepsilon = 0.15$ appear to be overly aggressive, as evidenced by the fact that the number of *Solved* cases is never maximized for this value.

Regardless of the choice of ε and the dimension n , the average post-heuristic gaps decrease significantly, while the number of cases yielding an *invalid* (upper) bound remains relatively small. Moreover, note that random instances from Table 2 with 20% zero entries appear to be harder to solve compared to the dense ones, as indicated by their relatively higher pre-heuristic gaps. Nonetheless, **H1** successfully reduces these gaps by at least half in seven out of eight parameter configurations.

Furthermore, we observe that moderate choices of the penalization factor, such as $\varepsilon = 0.05$ or $\varepsilon = 0.1$, typically solve the highest number of cases to optimality much before reaching the maximum number of iterations. In other words, for these values of ε , Algorithm 1 appears to be able to certify that further reductions of the feasible set are unnecessary, as they would either yield invalid (upper) bounds or fail to significantly reduce the gap.

Finally, we highlight the efficiency of **H1** compared to the computationally expensive second-order relaxation. For example, when $n = 30$ and $s = 20\%$, recovering the true optimal values using the second-order relaxation takes an average of 1163.134s. In contrast, Algorithm 1 with $\varepsilon = 0.1$ takes only 0.819s, solving 13 cases and reducing the average gap by half. Additionally, it is worth emphasizing that, despite requiring multiple iterations, **H1** remains much faster than solving the second-order relaxation.

The following figure illustrates the impact of the choice of penalization factor ε on the speed at which the relaxation bound improves:

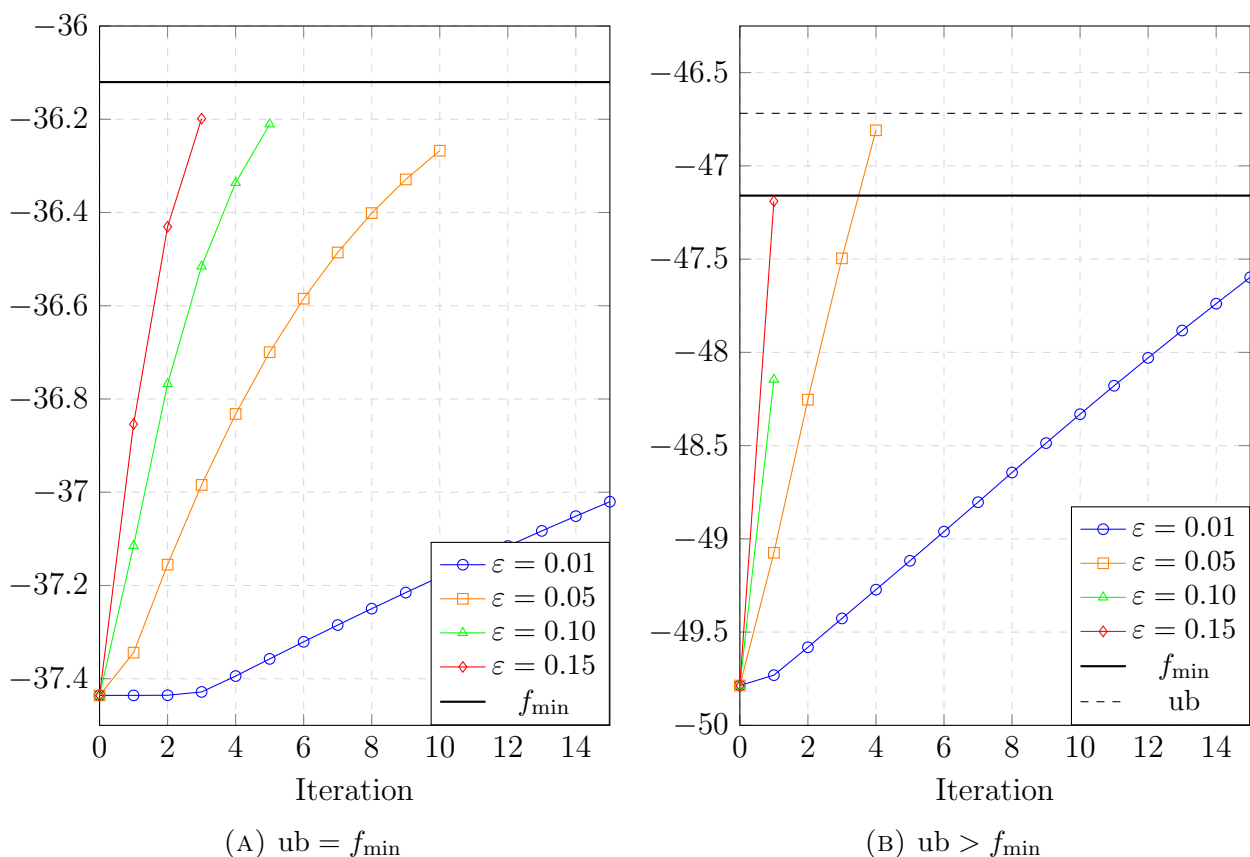


FIGURE 5. Trajectories $(\tilde{f}_{1,k})_{0 \leq k \leq 15}$ from Algorithm 1 for different values of ε , in dimension $n = 20$, with (\mathbf{Q}, \mathbf{q}) dense and randomly generated, using seeds 16 (left) and 38 (right).

The left subfigure of Figure 5 demonstrates that a valid lower bound was obtained for all tested values of ε . It also reveals that smaller values of ε reduce the speed at which the bound improves. In contrast, the right subfigure of Figure 5 shows a particular instance where an invalid (upper) bounds was obtained for $\varepsilon = 0.05$. Unlike the left subfigure, Algorithm 1 failed to recover a tight upper bound ub in this case, leading to inaccurate measurements of the relative optimality gap. Despite this issue, for more severe penalization factors, such as $\varepsilon = 0.15$ or $\varepsilon = 0.1$, **H1** was able to certify that for any $k \geq 2$, we must have $\tilde{f}_{1,k} > f_{\min}$. As a result, the best proposed bound $\tilde{f}_{1,1}$ satisfied $f_1 < \tilde{f}_{1,1} < f_{\min}$. Moreover, cautious reductions of the feasible set generally

avoid producing invalid (upper) bounds, though at the expense of requiring a higher number of iterations. This observation holds regardless of the availability of tight upper bounds.

4.1.2. *Performance of H2*. We continue by assessing the performance of **H2**, implemented via Algorithm 2. The kernel dimension of the marginal moment matrices was determined by counting the number of eigenvalues smaller than 10^{-3} . The regularization parameter for computing the marginal Christoffel sublevel sets was set to $\beta = 10^{-3}$.

n	s	τ	$\tilde{f}_1 > f_{\min}$	Gap (%)		Time (s)		Solved
				$\Delta(f_1, f_{\min})$	$\Delta(\tilde{f}_1, f_{\min})$	\tilde{f}_1	f_2	
20	0%	None	4	4.834	0.410	0.083	26.339	39
		1.5	4	4.834	0.588	0.086	26.339	35
		1.25	1	4.933	1.212	0.085	26.311	28
		1.1	0	4.934	2.314	0.094	26.268	19
	20%	None	7	4.317	0.268	0.026	26.793	38
		1.5	5	4.395	0.391	0.045	26.734	36
		1.25	1	4.740	0.878	0.044	26.560	29
		1.1	1	4.740	2.177	0.045	26.560	17
30	0%	None	11	5.092	0.525	0.304	1209.983	32
		1.5	6	5.453	0.757	0.296	1202.457	27
		1.25	4	5.566	1.484	0.306	1203.910	18
		1.1	2	5.527	2.781	0.323	1207.392	11
	20%	None	5	6.059	0.740	0.094	1172.473	30
		1.5	2	6.030	1.022	0.087	1167.344	29
		1.25	0	6.059	1.780	0.093	1163.134	12
		1.1	0	6.059	3.364	0.092	1163.134	5

TABLE 3. Performance of **H2** in dimensions 20 and 30, for different values of the filtering parameter τ (“None” corresponds to cases where no filtering is used).

Firstly, notice that the runtime of Algorithm 2 is usually smaller compared to the running time of Algorithm 1 over the same POP instances. This is due to the fact that Algorithm 2 requires only one iteration. However, Algorithm 2 is highly dependent on the quality of the available local solutions. For example, when $n = 30$ and $s = 0\%$, 15 out of 50 available local solutions yielded strict upper bounds, and Algorithm 2, without enabled filtering, provided invalid (upper) bounds in 11 out of those 15 cases.

The number of those undesirable scenarios can be reduced by cautiously filtering the sublevel constraints, which happens, for instance, when $\tau = 1.1$. However, this conservative approach yields significantly smaller average gap improvement, illustrating the trade-off between the risk of over-restriction and the possibility of highly significant bound improvements.

To summarize, both **H1** and **H2** effectively strengthen the bounds of moment relaxations while being significantly less computationally prohibitive than higher-order relaxations. The reductions of the feasible set induced by **H1** are gradual and thus more cautious, particularly for small values of ε . Due to the weaker dependence of **H1** on the quality of available upper bounds, we conjecture that **H1** would be preferable for general classes of more challenging problems, where obtaining high-quality locally optimal solutions is difficult. Conversely, for specific classes of POP problems where high-quality local solutions are readily available, strengthening the bounds via **H2** would be a highly reasonable approach.

4.2. Exploiting correlative sparsity. So far, we have only considered POP instances that present no underlying structure that could be leveraged to increase the efficiency of the associate SDP solving procedure. However, many optimization problems possess important structural properties, such as sparsity. In this subsection, we focus on *correlative sparsity* [31, 14] and demonstrate the efficiency of our proposed approaches within this framework.

Before presenting our experimental results, let us provide a short reminder of the correlative-sparsity-based Moment-SOS hierarchy.

Let us suppose that $\{1, \dots, n\} =: I_0 = \cup_{l=1}^p I_l$ with I_l not necessarily disjoint and let $n_l = |I_l|$. To each subset I_l , we can associate the corresponding subset of decision variables $\mathbf{x}_{I_l} := \{x_i, i \in I_l\}$. We say that an instance of POP exhibits correlative sparsity if

- There exist $(f_l)_{l \in \{1, \dots, p\}}$ such that $f = \sum_{l=1}^p f_l$, with $f_l \in \mathbb{R}[\mathbf{x}_{I_l}]$,
- The polynomials $(g_j)_{j \in \{1, \dots, m\}}$ can be split into disjoint sets J_l , such that $g_j \in J_l$ if and only if $g_j \in \mathbb{R}[\mathbf{x}_{I_l}]$.

Then, the *correlatively sparse moment relaxation* of order $d \geq d_{\min}$ is given by:

$$(38) \quad \mathbf{P}_d^{\text{cs}} : \begin{cases} f_d^{\text{cs}} := \inf_{\mathbf{y}_l \in \mathbb{R}^{\mathbb{N}_{2d}^{n_l}}} \sum_{l=1}^p L_{\mathbf{y}_l}(f_l) \\ \text{s.t.} & \mathbf{M}_d(\mathbf{y}_l) \in \mathcal{S}_+^{s(n_l, d)}, \quad l \in \{1, \dots, p\}, \\ & \mathbf{M}_{d-d_j}(g_j \mathbf{y}_l) \in \mathcal{S}_+^{s(n_l, d-d_j)}, \quad j \in J_l, \quad l \in \{1, \dots, p\}, \\ & L_{\mathbf{y}_l}(1) = 1, \quad l \in \{1, \dots, p\}, \end{cases}$$

where we let $\mathbf{y}_l := \{y_\alpha \mid \alpha \in \mathbb{N}_{2d}^n, \forall i \in \{1, \dots, s(n, d)\}, \alpha_i = 0, \forall i \notin I_l\}$. The corresponding SOS relaxation can be built analogously. A detailed convergence analysis of the hierarchy from (38) is available in [14].

Notice that, if $\rho := \max_{l \in \{1, \dots, p\}} n_l$, then SDP relaxations from (38) contain matrices of maximum size

$s(\rho, d) = \mathcal{O}(\rho^d)$, yielding a significant improvement when $\rho \ll n$. However, given a relaxation order $d \geq d_{\min}$, the bound f_d^{cs} can be arbitrarily far from f_{\min} . In high-dimensional settings, where even the size of ρ is not negligible, improving the bound by ascending the hierarchy (e.g., computing f_{d+1}^{cs} , f_{d+2}^{cs} , and so on) remains a significant computational challenge. Nonetheless, we demonstrate that our proposed approaches are capable of providing strengthened bounds \tilde{f}_d^{cs} within this framework.

Remark 4.1. Both **H1** and **H2** can be efficiently integrated with correlative sparsity exploitation. The modified versions, referred to as **H1CS** and **H2CS**, are detailed in the [Appendix](#).

Let us consider the following optimization problem:

$$(39) \quad \min_{\mathbf{x} \in \mathbb{R}^n} \left\{ \mathbf{x}^\top \mathbf{q} + \sum_{l=1}^p \mathbf{x}_{I_l}^\top \mathbf{Q}_l \mathbf{x}_{I_l} \mid \mathbf{0} \leq \mathbf{x} \leq \mathbf{1} \right\},$$

where $\mathbf{Q}_l \in \mathcal{S}^{n_l}$ for each $l \in \{1, \dots, p\}$, $\mathbf{q} \in \mathbb{R}^n$, and $n = \sum_{l=1}^p n_l - \sum_{l=1}^{p-1} |I_l \cap I_{l+1}|$. We suppose that $|I_l \cap I_{l+1}| > 0$ for all $l \in \{1, \dots, p-1\}$.

Notice that POP instances of the form (39) possess a correlatively sparse structure by construction. These instances can also be written in the form (37), where the matrix $\mathbf{Q} \in \mathcal{S}^n$ is block-diagonal, having p blocks, with each block associated with a distinct subset I_l . Moreover, solving optimization problems of this form naturally arises in many applications, such as portfolio optimization [5] or classification via support vector machines [17].

We generate 50 such POP instances using the following structure: $p = 7$, $n_l = 22$ for $l \in \{1, \dots, p\}$, and $|I_l \cap I_{l+1}| = 4$ for $l \in \{1, \dots, p-1\}$. Consequently, we get $n = 130$. We set $\delta = 0.5\%$ and $\beta = 10^{-4}$. Obtained results are presented in Table 4 and Table 5.

n	ε	$\tilde{f}_1^{\text{cs}} > f_{\min}$	Gap (%)		Time (s)		Solved	k
			$\Delta(f_1^{\text{cs}}, f_{\min})$	$\Delta(\tilde{f}_1^{\text{cs}}, f_{\min})$	\tilde{f}_1^{cs}	f_2^{cs}		
125	0.01	0	5.890	4.670	2.939	468.294	0	15.00
	0.05	10	5.757	1.359	2.706	469.012	15	13.12
	0.1	13	5.764	0.551	1.650	466.427	21	8.35
	0.15	11	5.661	1.073	1.080	468.437	12	5.15
	0.25	8	5.851	1.808	0.952	469.787	8	2.69

TABLE 4. Performance of **H1CS** for different values of the penalization factor ε , and randomly generated input data. The number of cases where **H1CS** has access only to a strict upper bound is 41 out of 50.

Firstly, notice that, despite correlative sparsity exploitation, second-order moment relaxation remains costly with respect to **H1CS**. Moreover, **H1CS** effectively reduces the optimality gaps in all considered configurations. Given the high-dimensionality of the problem, a more severe penalization, like $\varepsilon = 0.25$, also seems efficient in reducing the gaps while maintaining the number of wrong cases relatively small.

n	τ	$\tilde{f}_1^{\text{cs}} > f_{\min}$	Gap (%)		Time (s)		Solved
			$\Delta(f_1, f_{\min})$	$\Delta(\tilde{f}_1^{\text{cs}}, f_{\min})$	\tilde{f}_1^{cs}	f_2^{cs}	
125	None	5	5.955	0.625	0.252	468.635	24
	1.5	0	5.890	0.873	0.208	468.294	11
	1.25	0	5.890	1.814	0.217	468.294	2
	1.1	0	5.890	3.387	0.216	468.294	0

TABLE 5. Performance of **H2CS** for different values of the filtering parameter τ , and randomly generated input data. The available local solution $\bar{\mathbf{x}}$ is not global, i.e., $f(\bar{\mathbf{x}}) > f_{\min}$, in 41 out of 50 cases.

As demonstrated in Table 5, **H2CS** appears to be capable of efficiently taking advantage of the information provided by available locally optimal solutions. Furthermore, we observe similar trade-offs as those observed in the absence of correlative sparsity, see Table 3. Significantly reduced gaps and a low number of unsuccessful cases further highlight an important observation: the locally optimal solutions provided by Ipopt are generally quite close to the globally optimal solutions. Generally speaking, since the first-order relaxation in these cases is not extremely loose, **H2CS** can be understood as assessing the quality of given locally optimal solutions.

4.3. Beyond QCQPs. Optimization problems analyzed earlier are quadratic and addressed using first-order (sparse) Moment-SOS relaxation, with our approaches effectively strengthening bounds. However, many POPs involve higher-degree polynomials (e.g., cubic or quartic), necessitating higher-order relaxations. We illustrate the integration of our approaches in such relaxations with the following example.

Let $\mathbf{Q} \in \mathcal{S}^n$, $\mathbf{q} \in \mathbb{R}^n$, $(r_1, r_2) \in \mathbb{R}_+ \times \mathbb{R}_+$, $(\mathbf{c}_1, \mathbf{c}_2) \in \mathbb{R}^n \times \mathbb{R}^n$. Let $g_1 : \mathbf{x} \mapsto r_1^2 - \|\mathbf{x} - \mathbf{c}_1\|_2^2$ and $g_2 : \mathbf{x} \mapsto r_2^2 - \|\mathbf{x} - \mathbf{c}_2\|_2^2$. Consider the following optimization problem:

$$(40) \quad \min_{\mathbf{x} \in K} f(\mathbf{x}) := \mathbf{x}^\top \mathbf{Q} \mathbf{x} + \mathbf{x}^\top \mathbf{q},$$

where $K = \{\mathbf{x} \in \mathbb{R}^n \mid -g_1(\mathbf{x})g_2(\mathbf{x}) \geq 0\}$.

Optimization problems of this form consist of minimizing a quadratic (nonconvex) function over a nonconvex set corresponding to the union of two Euclidian balls. This is a quartic optimization problem, as the feasible set is described using a polynomial of degree four. Consequently, the minimal order relaxation is the relaxation of order two.

We consider the following configuration: $n = 5$, $(r_1, r_2) = (1.0, \sqrt{0.1})$, $(\mathbf{c}_1, \mathbf{c}_2) = (\mathbf{0}, \mathbf{1})$, and

$$\mathbf{Q} = \begin{bmatrix} -1.4396 & -0.2259 & 0.0983 & -0.0085 & -2.3838 \\ -0.2259 & 0.8043 & 0.3730 & 1.2719 & 0.1370 \\ 0.0983 & 0.3730 & -1.0236 & 0.0597 & 0.5024 \\ -0.0085 & 1.2719 & 0.0597 & 0.9421 & 1.2085 \\ -2.3838 & 0.1370 & 0.5024 & 1.2085 & 0.7885 \end{bmatrix}, \quad \mathbf{q} = \begin{bmatrix} -1.269 \\ -2.988 \\ 2.535 \\ -0.4151 \\ 0.1464 \end{bmatrix}.$$

For this particular POP, we have $f_{\min} = f_3 = -5.7161$, and $f_2 = -7.3367$, so that $\Delta(f_2, f_{\min}) = 22.90\%$. We also have $\mathbf{x}^* = (0.6252, 0.4015, -0.5397, -0.1415, 0.3697)$.

Performance of H1. Let us denote by $\tilde{f}_{d,d_c,k}$ the output of **H1** at iteration $k \geq 1$, where $d_c \in \{1, \dots, d\}$ is the degree of Christoffel polynomials used for modifying the feasible set. Then, there are two possible ways in which our iterative approach can be coupled with high-order relaxations.

- Firstly, one can modify the feasible set using the Christoffel polynomials constructed from pseudo-moment matrices of order d . As the higher-order pseudo-moment matrices contain information about monomials of higher degrees, the resulting sublevel sets, possibly nonconvex, are expected to be much more precise, a phenomenon that has already been described in Figure 1. Consequently, the number of iterations to reach satisfactory bound improvements should intuitively be smaller. For the optimization problem in (40), we obtain $\tilde{f}_{2,2,5} = -6.7029$, yielding $\Delta(\tilde{f}_{2,2,5}, f_{\min}) = 14.72\%$.
- Secondly, from the pseudo-moment matrix of order d , one can extract a submatrix of order $d_c < d$, and modify the feasible set using less complicated level sets of low order Christoffel polynomials. This can be beneficial, for example, in high-dimensional

settings, where construction of high-degree Christoffel polynomials can be challenging.

In the particular case of (40), we get $\tilde{f}_{2,1,5} = -6.6961$, so that $\Delta(\tilde{f}_{2,1,5}, f_{\min}) = 14.64\%$.

Our numerical experiments highlight the significant role of polynomials in the kernel of pseudo-moment matrices for $d \geq 2$. This should be carefully considered when $d_c = d$, as it requires an appropriate adjustment of β . For instance, second-order relaxation generally appears less accurate for problems with nonconvex and/or disconnected feasible sets, such as (40). As a result, even second-order Christoffel polynomials may fail to accurately capture the true location of the minimizer, particularly when β is set very close to zero. In contrast, selecting $d_c = 1$, appears to be a more conservative approach for reducing the size of the feasible set, typically yielding slower improvements in the bounds. Hence, without prior knowledge of higher-order relaxation quality, applying the bound-strengthening technique with $d_c = 1$ is a safer and effective approach.

Performance of H2. We remind that **H2** is always applied using the marginal Christoffel polynomials with $d_c = 1$. In case of higher-order relaxations, we expect the pseudo-moment matrices to contain more information, which, in turn, can increase the efficiency of **H2**. The available local solution is $\bar{\mathbf{x}} = (1.2602, 0.9712, 0.9292, 0.8395, 1.0262)$.

After constructing the five marginal Christoffel polynomials, we obtain the following list of candidate thresholds (see (30)) :

$$(\lambda_1, \lambda_2, \lambda_3, \lambda_4, \lambda_5) = (1.2059, 2.5729, 4.2559, 8.3069, 1.5804).$$

Hence, by setting $\tau = 1.5$, the algorithm **H2** applies the feasible set reduction with respect to the first coordinate only, yielding a new bound $\tilde{f}_{2,1} = -6.1883$, and a new optimality gap $\Delta(\tilde{f}_{2,1}, f_{\min}) = 7.63\%$. Using smaller values of the threshold filtering parameter τ leaves the initial relaxation bound f_2 unchanged.

5. CONCLUSION

To mitigate the computational complexity of high-order SOS-relaxations, our paper shows that it is possible to enhance the accuracy of low-order relaxations by leveraging Christoffel-Darboux kernels. Specifically, we propose two distinct algorithms aimed at obtaining tighter lower bounds at order d of the hierarchy, exploiting only the information available at this order. Our first approach, denoted as **H1**, is an iterative procedure designed to enhance the bounds by systematically eliminating suboptimal solutions. In contrast, our second approach, **H2**, focuses on leveraging the quality of available local solutions to efficiently reduce the size of the feasible set, thereby improving the lower bounds.

Our experimental results demonstrate the advantages of these two approaches, particularly for various types of QCQPs, where they often yield significantly improved lower bounds up to $1000\times$ faster than solving the computationally expensive higher-order relaxations. We also introduced **H1CS** and **H2CS**, which are refinements of **H1** and **H2**, designed to exploit correlative sparsity. Despite the inherently sparse structure of many POP instances, ascending the hierarchy remains challenging. Nevertheless, our heuristic approaches consistently improve the bounds in these scenarios.

In many real-life scenarios, access to tight lower bounds is of paramount importance. This motivates our belief that a more general study of bound-strengthening approaches, similar to ours, could significantly enhance the solving times of SDP relaxations. For instance, incorporating our heuristic bounds within a general-purpose Branch & Bound solver could potentially reduce solving times by minimizing the number of necessary branchings. A potential generalization of our work could involve developing an adaptive selection scheme for the threshold penalization factor in **H1** and **H1CS**, the aim being to impose less stringent penalizations in scenarios where a reduction in the rank of the moment matrices is observed. Finally, extending our

approaches to more general POP instances, such as those with discrete constraints, constitutes an interesting direction for future research.

ACKNOWLEDGEMENTS

This work was supported by the European Union’s HORIZON–MSCA-2023-DN-JD programme under the Horizon Europe (HORIZON) Marie Skłodowska-Curie Actions, grant agreement 101120296 (TENORS), the AI Interdisciplinary Institute ANITI funding, through the French “Investing for the Future PIA3” program under the Grant agreement n° ANR-19-PI3A-0004 as well as by the National Research Foundation, Prime Minister’s Office, Singapore under its Campus for Research Excellence and Technological Enterprise (CREATE) programme. This work was partially performed using HPC resources from CALMIP (Grant 2023-P23035).

REFERENCES

- [1] Erling D Andersen and Knud D Andersen. The MOSEK interior point optimizer for linear programming: an implementation of the homogeneous algorithm. In *High performance optimization*, pages 197–232. Springer, 2000.
- [2] Raúl Curto and Lawrence Fialkow. The truncated complex k-moment problem. *Transactions of the American mathematical society*, 352(6):2825–2855, 2000.
- [3] Charles F Dunkl and Yuan Xu. *Orthogonal polynomials of several variables*, volume 155. Cambridge University Press, 2014.
- [4] Bissan Ghaddar, Juan C Vera, and Miguel F Anjos. A dynamic inequality generation scheme for polynomial programming. *Mathematical Programming*, 156:21–57, 2016.
- [5] Jacek Gondzio and Andreas Grothey. Parallel interior-point solver for structured quadratic programs: Application to financial planning problems. *Annals of Operations Research*, 152(1):319–339, July 2007.
- [6] Didier Henrion, Milan Korda, and Jean Bernard Lasserre. *The Moment-SOS Hierarchy*. WORLD SCIENTIFIC (EUROPE), 2020.
- [7] Didier Henrion and Jean-Bernard Lasserre. Detecting global optimality and extracting solutions in gloptipoly. In *Positive polynomials in control*, pages 293–310. Springer, 2005.
- [8] Cédric Jozs and Didier Henrion. Strong duality in lasserre’s hierarchy for polynomial optimization. *Optimization Letters*, 10(1):3–10, 2016.
- [9] Milan Korda, Monique Laurent, Victor Magron, and Andries Steenkamp. Exploiting ideal-sparsity in the generalized moment problem with application to matrix factorization ranks. *Mathematical Programming*, 205(1):703–744, May 2024.
- [10] András Kroó and Doron S. Lubinsky. Christoffel functions and universality in the bulk for multivariate orthogonal polynomials. *Canadian Journal of Mathematics*, 65(3):600–620, 2013.
- [11] J.B. Lasserre, E. Pauwels, and M. Putinar. *The Christoffel–Darboux Kernel for Data Analysis*. Cambridge Monographs on Applied and Computational Mathematics. Cambridge University Press, 2022.
- [12] Jean B Lasserre. Global optimization with polynomials and the problem of moments. *SIAM Journal on optimization*, 11(3):796–817, 2001.
- [13] Jean B. Lasserre. The Christoffel function: Applications, connections and extensions. *Numerical Algebra, Control and Optimization*, 2024.
- [14] Jean-Bernard Lasserre. Convergent SDP-Relaxations in Polynomial Optimization with Sparsity. *Siam Journal on Optimization*, 17:263–272, 01 2006.
- [15] Jean Bernard Lasserre, Edouard Pauwels, and Mihai Putinar. *The Christoffel–Darboux Kernel for Data Analysis*, volume 38. Cambridge University Press, 2022.
- [16] Monique Laurent. Sums of squares, moment matrices and optimization over polynomials. In *Emerging applications of algebraic geometry*, pages 157–270. Springer, 2009.
- [17] Ching-Pei Lee and Dan Roth. Distributed box-constrained quadratic optimization for dual linear svm. *Proceedings of the 32nd International Conference on International Conference on Machine Learning - Volume 37*, page 987–996, 2015.
- [18] Victor Magron and Jie Wang. TSSOS: a Julia library to exploit sparsity for large-scale polynomial optimization. *ArXiv*, abs/2103.00915, 2021.
- [19] Victor Magron and Jie Wang. *Sparse Polynomial Optimization*. WORLD SCIENTIFIC (EUROPE), 2023.
- [20] Swann Marx, Edouard Pauwels, Tillmann Weisser, Didier Henrion, and Jean Bernard Lasserre. Semi-algebraic approximation using christoffel–darboux kernel. *Constructive Approximation*, 54(3):391–429, Dec 2021.

- [21] Paul Nevai. Géza freud, orthogonal polynomials and christoffel functions. a case study. *Journal of approximation theory*, 48(1):3–167, 1986.
- [22] Jiawang Nie. Optimality conditions and finite convergence of lasserre’s hierarchy. *Mathematical Programming*, 146(1):97–121, Aug 2014.
- [23] Jiawang Nie. Tight relaxations for polynomial optimization and lagrange multiplier expressions. *Mathematical Programming*, 178(1):1–37, Nov 2019.
- [24] Jiawang Nie. *Moment and Polynomial Optimization*. Society for Industrial and Applied Mathematics, Philadelphia, PA, 2023.
- [25] Edouard Pauwels and Jean B Lasserre. Sorting out typicality with the inverse moment matrix sos polynomial. In D. Lee, M. Sugiyama, U. Luxburg, I. Guyon, and R. Garnett, editors, *Advances in Neural Information Processing Systems*, volume 29. Curran Associates, Inc., 2016.
- [26] Mihai Putinar. Positive polynomials on compact semi-algebraic sets. *Indiana University Mathematics Journal*, 42(3):969–984, 1993.
- [27] Zheng Qu and Xindong Tang. A correlatively sparse lagrange multiplier expression relaxation for polynomial optimization. *SIAM Journal on Optimization*, 34(1):127–162, 2024.
- [28] Cordian Riener, Thorsten Theobald, Lina Jansson Andrén, and Jean B. Lasserre. Exploiting symmetries in sdp-relaxations for polynomial optimization. *Mathematics of Operations Research*, 38(1):122–141, 2013.
- [29] Barry Simon. The christoffel-darboux kernel. In *Perspectives in PDE, Harmonic Analysis and Applications,” a volume in honor of VG Maz’ya’s 70th birthday, Proceedings of Symposia in Pure Mathematics*, volume 79, pages 295–335, 2008.
- [30] Andreas Wächter and Lorenz T. Biegler. On the implementation of an interior-point filter line-search algorithm for large-scale nonlinear programming. *Mathematical Programming*, 106(1):25–57, 2006.
- [31] Hayato Waki, Sunyoung Kim, Masakazu Kojima, and Masakazu Muramatsu. Sums of squares and semi-definite program relaxations for polynomial optimization problems with structured sparsity. *SIAM Journal on Optimization*, 17(1):218–242, 2006.
- [32] Jie Wang. Strengthening lasserre’s hierarchy in real and complex polynomial optimization, 2024.
- [33] Jie Wang, Haokun Li, and Bican Xia. A new sparse sos decomposition algorithm based on term sparsity. In *Proceedings of the 2019 International Symposium on Symbolic and Algebraic Computation, ISSAC ’19*, page 347–354, New York, NY, USA, 2019. Association for Computing Machinery.
- [34] Jie Wang, Victor Magron, and Jean-Bernard Lasserre. Tssos: A moment-sos hierarchy that exploits term sparsity. *SIAM Journal on Optimization*, 31(1):30–58, 2021.
- [35] Jianting Yang, Srećko Đurašinović, Jean-Bernard Lasserre, Victor Magron, and Jun Zhao. Verifying properties of binary neural networks using sparse polynomial optimization. *International Conference on Learning Representations*, 2025.

APPENDIX

For the sake of completeness, we present updated versions of Algorithm 1 and Algorithm 2 that are designed to be compatible with the exploitation of correlative sparsity.

Algorithm 3 Implementing **H1CS**

Input: Relaxation order d , gap tolerance $\delta > 0$, maximum number of iterations N , and a penalization factor $\varepsilon \in (0, 1)$.

Initialize: $k = 0$

- (1) Initialize the feasible set $\tilde{K}_k = K$.
- (2) Solve the *sparse* moment relaxation of order d . Recover its optimal solution $(\mathbf{y}_{l,k}^*)_{l \in \{1, \dots, p\}}$, relaxation bound $\tilde{f}_{d,k}^{\text{cs}} = f_d^{\text{cs}}$, and a local solution $\bar{\mathbf{x}}_k$ yielding an upper bound $\text{ub}_k = f(\bar{\mathbf{x}}_k)$.
- (3) Initialize the relative gap $\Delta_k = \Delta(f(\bar{\mathbf{x}}_k), \tilde{f}_{d,k}^{\text{cs}})$.

While $k < N$

- (4) **If** $\tilde{f}_{d,k}^{\text{cs}} > \text{ub}_k$ **or** $\Delta_k \leq \delta$:
 – **Break.**

- (5) For each $l \in \{1, \dots, p\}$, compute the Christoffel polynomials $\tilde{\Lambda}_d^{\mathbf{y}_{l,k}^*}$ and set $\gamma_{l,k} = L_{\mathbf{y}_{l,k}^*}(\tilde{\Lambda}_d^{\mathbf{y}_{l,k}^*})$.

- (6) Modify the feasible set via $\tilde{K}_{k+1} = \tilde{K}_k \cap \bigcap_{l \in \{1, \dots, p\}} \tilde{S}_d(\mathbf{y}_{l,k}^*, (1 - \varepsilon)\gamma_{l,k})$, and solve the

sparse moment relaxation of order d . Recover the new relaxation bound $\tilde{f}_{d,k+1}^{\text{cs}}$, the new optimal solution $(\mathbf{y}_{l,k+1}^*)_{l \in \{1, \dots, p\}}$, and the new locally optimal solution $\bar{\mathbf{x}}_{k+1}$.

- (7) Set $\text{ub}_{k+1} = \min_{i \in \{0, k+1\}} \{f(\bar{\mathbf{x}}_i)\}$ and re-evaluate the gap $\Delta_{k+1} = \Delta(\text{ub}_{k+1}, \tilde{f}_{d,k+1}^{\text{cs}})$.

- (8) Update the iteration count $k = k + 1$.

Output: Sequence of bounds $(\tilde{f}_{d,k}^{\text{cs}})_{k \geq 1}$ satisfying $\tilde{f}_{d,k+1}^{\text{cs}} \geq \tilde{f}_{d,k}^{\text{cs}} \geq f_d^{\text{cs}}$.

Algorithm 4 Implementing **H2CS**

Input: Relaxation order d , parameter $\tau > 1$.

- (1) Solve the *sparse* moment relaxation of order d . Recover its optimal solution $(\mathbf{y}_l^*)_{l \in \{1, \dots, p\}}$ and a local solution $\bar{\mathbf{x}}$.

- (2) For each $l \in \{1, \dots, p\}$, and for each $i \in I_l$, construct the marginal Christoffel polynomials $\tilde{\Lambda}_1^{\mathbf{y}_{l,[i]}^*}$ and compute the thresholds $\gamma_i = \tilde{\Lambda}_1^{\mathbf{y}_{l,[i]}^*}(\bar{\mathbf{x}}_i)$.

- (3) Modify the feasible set via $\tilde{K} = K \cap \bigcap_{\substack{l \in \{1, \dots, p\} \\ i \in I_l}} \{\mathbf{x} \in \mathbb{R}^n \mid x_i \in \tilde{S}_1(\mathbf{y}_{l,[i]}^*, \gamma_i)\}$, and solve

the *sparse* moment relaxation of order d .

Output: Tightened bound $\tilde{f}_d^{\text{cs}} \geq f_d^{\text{cs}}$.
